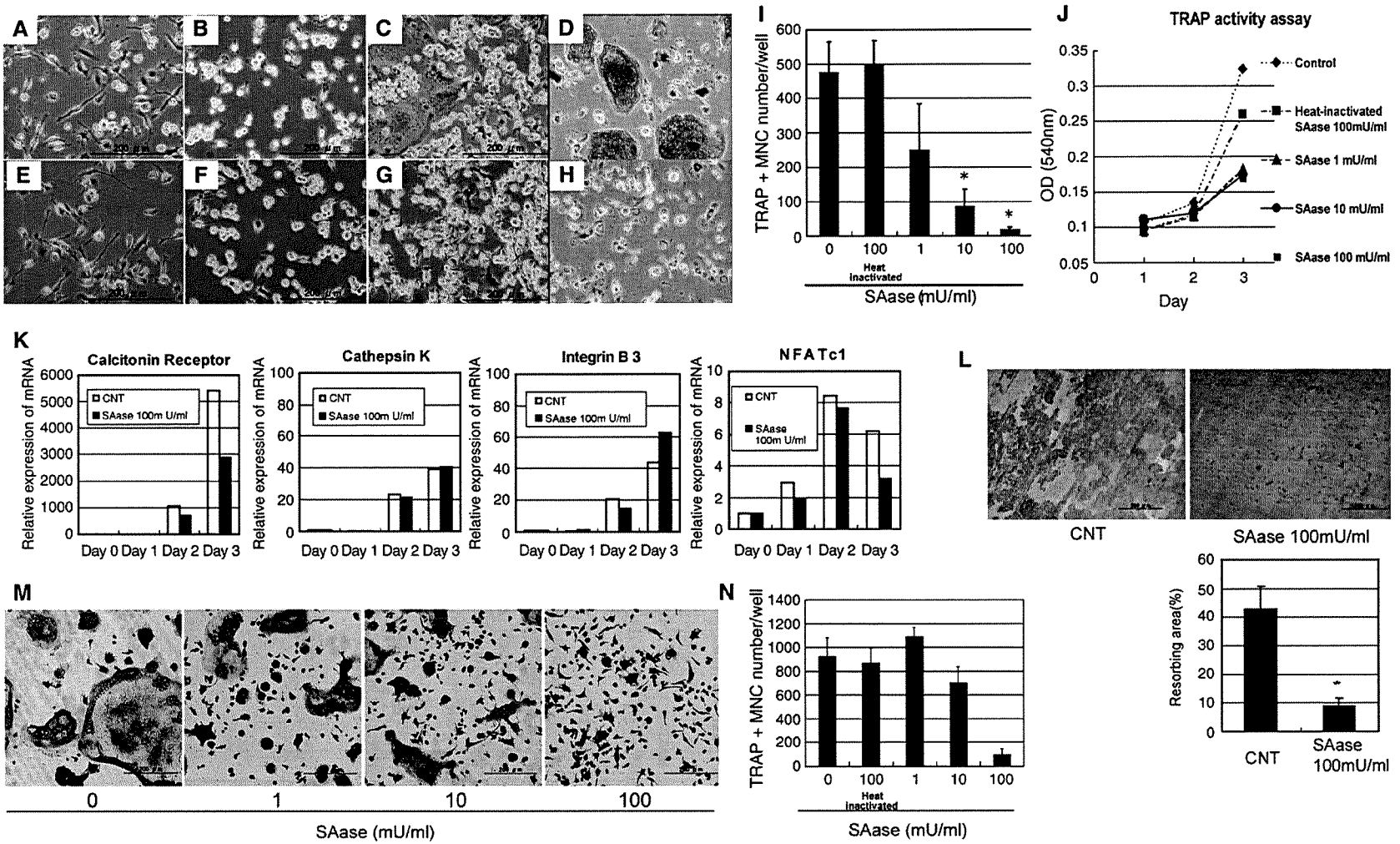

Fig. 4. (A–H) Differentiation of BMMs into mature osteoclasts. (A–D) Micrograph of mock-treated BMM cells. (E–H) Micrograph of 100 mU/ml SAase-treated BMM cells. Cells were cultured in the presence of rhM-CSF (30 ng/ml) and sRANKL (100 ng/ml) for 1 day (A and E), 2 days (B and F), and 3 days (C, D, G, and H). TRAP staining of mock or SAase-treated BMM cells after 3-day culture are shown (D or H). Original magnification, ×100. (I) Differentiation efficiency of BMM cells into TRAP-positive MNCs is shown. After 3-day culture, the number of TRAP-positive MNCs in each well of the 48-well plates was counted. (J) TRAP activity of BMM cell culture supernatant during osteoclastogenesis is shown. (K) Effect of desialylation of osteoclast precursor cells on mRNA expression of osteoclast markers during osteoclastogenesis. Calcitonin receptor, cathepsin K, integrin β3, and NFATc1 in osteoclast differentiation of BMM cells stimulated with rhM-CSF (30 ng/ml) and sRANKL (100 ng/ml). Mean values of three examinations are shown. (L) Formation of resorption pits by differentiated BMMs with or without 100 mU/ml SAase treatment in the presence of rhM-CSF (30 ng/ml) and sRANKL (100 ng/ml) for 10 days on dentin slices in 48-well plates. Original magnification, ×100. Efficacy of resorption activity of differentiated BMM cells. Slices were stained with hematoxylin and the area of the resorption pit on a dentin slice was calculated. (M) Inhibitory effect of desialylation of cell surface glycoconjugates on osteoclast differentiation in RAW 264.7 cells. Photograph of TRAP staining RAW 264.7 cells stimulated with sRANKL (50 ng/ml) after 5 days in 48-well plates, treated with SAase (0 mU/ml, 1 mU/ml, 10 mU/ml, or 100 mU/ml). Original magnification, ×100. (N) Differentiation efficacy of RAW 264.7 cells into TRAP-positive MNCs. Data are expressed as the mean and SD of the three cultures. (*, statistically different from mock-treated cells, $P<0.05$).

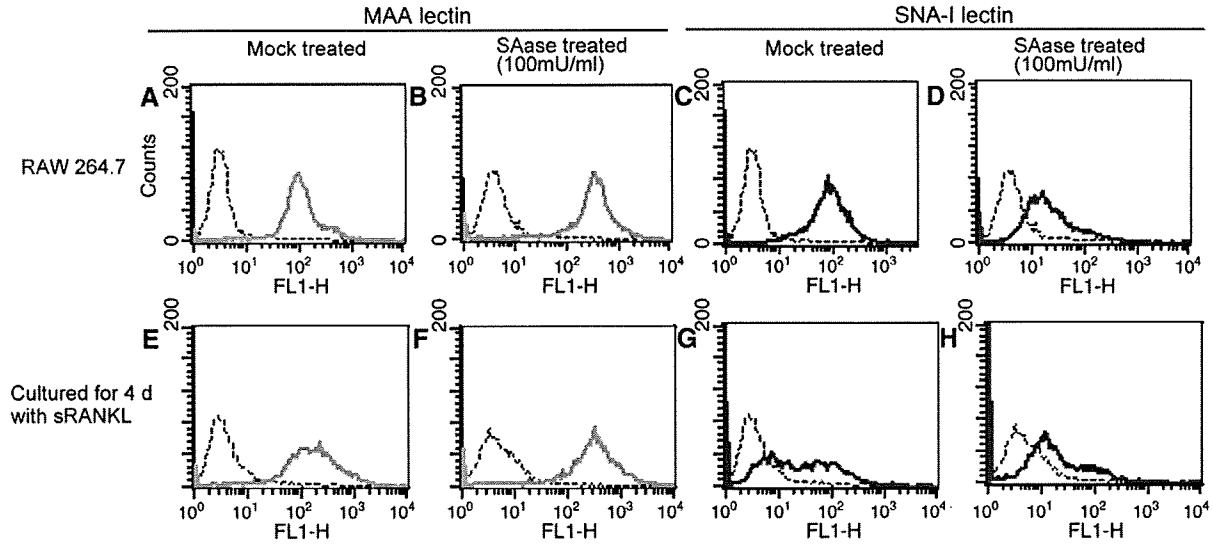

Fig. 5. Flow cytometric analyses of surface MAA lectin staining for alpha (2,3)-linked-sialic acid (A, B, E, F) and SNA-I lectin staining for alpha (2,6)-linked-sialic acid (C, D, G, H) during osteoclastogenesis with or without SAase treatment. (A–D) Upper panels show RAW264.7 cells as osteoclast precursors. (E–H) Lower panels show RAW 264.7 cells stimulated with sRANKL (50 ng/ml) after 4 days. (A, E, C, G) Mock-treated cells. (B, F, D, H) 100 mU/ml SAase-treated cells.

osteoclast precursor cells is a member of the tissue necrosis factor receptor family that encodes a 625-amino acid residue type I transmembrane protein with two potential N-linked glycosylation sites. Therefore, sialylation of RANK glycoconjugates might affect the RANKL/RANK signaling function [1]. RANKL-induced mRNA expression of osteoclast marker genes, however, was normal and TRAP-positive mononuclear cellswere formed from SAase-treated cells. Consequently, we concluded that the removal of sialic acid from cell surface glycoconjugates does not affect M-CSF or RANKL signaling in osteoclast differentiation.

It is worth mentioning that another sugar chain is involved in osteoclast cell–cell fusion. High-mannose type oligosaccharide and mannose receptors are both expressed on the cell surface of osteoclast precursors and mediate osteoclast cell–cell fusion [16,22]. The sialic acid mediated cell–cell fusion mechanism uncovered in this study is not involved in this high-mannose type oligosaccharide mediated cell–cell fusion mechanism. High-mannose type oligosaccharide does not contain sialic acid. Furthermore, Morishima et al. also reported that mannosidase I inhibitor, which inhibits the formation of complex type and hybrid type N-linked oligosaccharides that contain sialic acid, increases the formation of TRAP-positive MNCs in an osteoclastogenesis assay.

The results of this study suggested that quantitative and linkage-specific differences in sialylation of cell surface glycoconjugates regulate osteoclastic differentiation; however, there is currently little available information regarding the mechanism underlying regulation of the sialic acid content in osteoclasts or osteoclast precursors. Sialyltransferases, which reside in the Golgi apparatus, add cytidine monophosphate-activated sialic acid residues to specific terminal nonreducing positions on oligosaccharide chains of protein and lipids, but mRNA expression of ST6Gal-I showed no significant change despite the decrease of alpha (2,6)-linked-sialic acid during osteoclastgenesis. This means that there is a mechanism that degrades alpha (2,6)-linked-sialic acid during osteoclast differentiation. One possible mechanism is that endogenous SAases, which comprise four distinct forms with a predominant cellular localization (lysosomal, cytosolic, or plasma

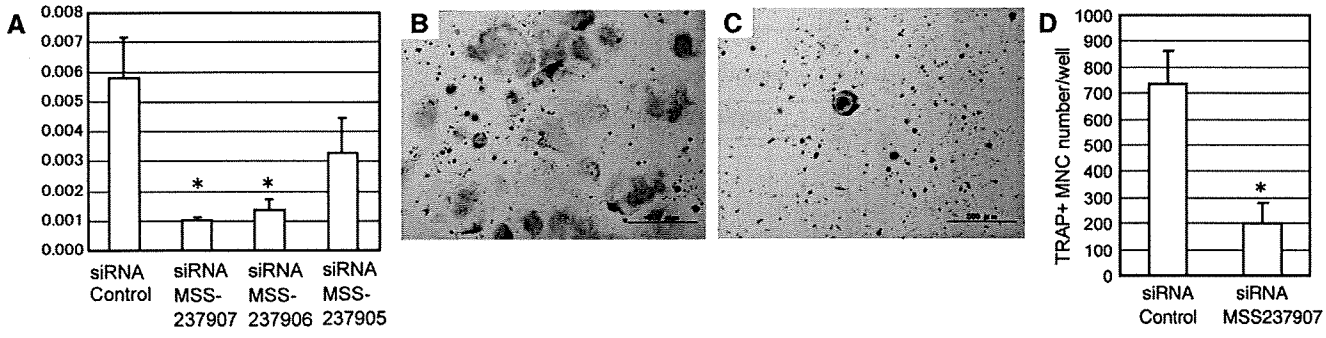

Fig. 6. Knock-down of ST6Gal-I in osteoclast precursors using siRNA and its effect on osteoclast differentiation. (A) mRNA expression level of ST6Gal-I in RAW264.7 cells at 72 h after siRNA transfection. (B) TRAP staining of RAW cells transfected with siRNA control and stimulated with sRANKL for 4 days. (C) TRAP staining of RAW cells transfected with siRNA MSS-237907 and stimulated with sRANKL for 4 days. (D) Differentiation efficiency of RAW cells into TRAP-positive MNCs is shown. Data are expressed as the mean and SD of the three experiments. (*, statistically different from siRNA control-treated cells, $P<0.05$).

membrane-associated), cleave sialic acid from glycoconjugates [21]. In monocyte/macrophage lineage cells, Stomatos et al. demonstrated the differential expression of endogenous SAases of human monocytes during cellular differentiation into macrophages [30]. However, in the differentiation process of osteoclast, there was no significant change in mRNA expression of mouse SAases (data not shown). Therefore, we speculate that alpha (2,6)-linked-sialic acid decreases as a result of the degradation or change in localization of cell surface glycoproteins or glycolipids that contains alpha (2,6)-linked-sialic acid during osteoclastgenesis. To elucidate the molecular mechanisms of alpha (2,6)-linked-sialic acid for osteoclast differentiation, further study of the regulation mechanism of the sialic acid content including identification of cell surface glycoproteins or glycolipids that contains alpha (2,6)-linked-sialic acid is necessary.

Overall, our findings demonstrate for the first time an essential role for sialic acid of cell surface glycoconjugates in the osteoclast differentiation process. Although the mechanism by which sialic acid mediates osteoclast differentiation remains unclear, alpha (2,6) linked-sialic acid is considered to be important for osteoclast cell–cell fusion. The results of this study will contribute to the future development of treatment options for bone diseases such as osteoporosis and rheumatoid arthritis.

Acknowledgments

Manufacturer Names: Wako Pure Chemical Industry Co., Ltd., Osaka, Japan; Becton Dickinson, Franklin Lakes, NJ; Corning Costar Inc., Corning, NY; Dojindo Laboratories, Kumamoto, Japan; Finnzymes Oy, Finland; Hokudo Co. Ltd., Japan; Meiji Seika, Tokyo, Japan; MJ Research, Hercules, CA; PeproTech EC, Ltd., London, U.K.; Nacalai Tesque, Inc., Kyoto, Japan; Pierce Biotechnology, Rockford, IL; Qiagen, Valencia, CA; Sigma Chemical Co., St. Louis, MO; EY Laboratories, San Mateo, CA; Cell Signaling, Beverly, MA.

References

[1] Anderson DM, Maraskovsky E, Billingsley WL, Dougall WC, Tometsko ME, Roux ER, et al. A homologue of the TNF receptor and its ligand enhance T-cell growth and dendritic-cell function. Nature 1997;390:175–9.

[2] Boyle WJ, Simonet WS, Lacey DL. Osteoclast differentiation and activation. Nature 2003;423:337–42.

[3] Bremer EG, Hakomori S, Bowen-Pope DF, Raines E, Ross R. Ganglioside-mediated modulation of cell growth, growth factor binding, and receptor phosphorylation. J Biol Chem 1984;259:6818–25.

[4] Crean SM, Meneski JP, Hullinger TG, Reilly MJ, DeBoever EH, Taichman RS. N-linked sialyated sugar receptors support haematopoietic cell-osteoblast adhesions. Br J Haematol 2004;124:534–46.

[5] Den H, Malinzak DA, Keating HJ, Rosenberg A. Influence of Concanavalin A, wheat germ agglutinin, and soybean agglutinin on the fusion of myoblasts in vitro. J Cell Biol 1975;67:826–34.

[6] Falzoni S, Chiozzi P, Ferrari D, Buell G, Di Virgilio F. P2X(7) receptor and polykarion formation. Mol Biol Cell 2000;11:3169–76.

[7] Ha H, Kwak HB, Lee SK, Na DS, Rudd CE, Lee ZH, et al. Membrane rafts play a crucial role in receptor activator of nuclear factor kappaB signaling and osteoclast function. J Biol Chem 2003;278:18573–80.

[8] Hartnell A, Steel J, Turley H, Jones M, Jackson DG, Crocker PR. Characterization of human sialoadhesin, a sialic acid binding receptor expressed by resident and inflammatory macrophage populations. Blood 2001;97:288–96.

[9] Hirohashi N, Vacquier VD. Egg sialoglycans increase intracellular pH and potentiate the acrosome reaction of sea urchin sperm. J Biol Chem 2002;277:8041–7.

[10] Illes T, Fischer J, Szabo G. Lectin histochemistry of pathological bones. Bull Hosp Jt Dis 1999;58:206–11.

[11] Ishii M, Iwai K, Koike M, Ohshima S, Kudo-Tanaka E, Ishii T, et al. RANKL-induced expression of tetraspanin CD9 in lipid raft membrane microdomain is essential for cell fusion during osteoclastogenesis. J Bone Miner Res 2006;21:965–76.

[12] Iwamoto T, Fukumoto S, Kanaoka K, Sakai E, Shibata M, Fukumoto E, et al. Lactosylceramide is essential for the osteoclastogenesis mediated by macrophage-colony-stimulating factor and receptor activator of nuclear factor-kappa B ligand. J Biol Chem 2001;276:46031–8.

[13] Keppler OT, Hinderlich S, Langner J, Schwartz-Albiez R, Reutter W, Pawlita M. UDP-GlcNAc 2-epimerase: a regulator of cell surface sialylation. Science 1999;284:1372–6.

[14] Keppler OT, Peter ME, Hinderlich S, Moldenhauer G, Stehling P, Schmitz I, et al. Differential sialylation of cell surface glycoconjugates in a human B lymphoma cell line regulates susceptibility for CD95 (APO-1/Fas)-mediated apoptosis and for infection by a lymphotropic virus. Glycobiology 1999;9:557–69.

[15] Kukita T, Wada N, Kukita A, Kakimoto T, Sandra F, Toh K, et al. RANKL-induced DC-STAMP is essential for osteoclastogenesis. J Exp Med 2004;200:941–6.

[16] Kurachi T, Morita I, Oki T, Ueki T, Sakaguchi K, Enomoto S, et al. Expression on outer membranes of mannose residues, which are involved in osteoclast formation via cellular fusion events. J Biol Chem 1994;269:17572–175876.

[17] Mbalaviele G, Chen H, Boyce BF, Mundy GR, Yoneda T. The role of cadherin in the generation of multinucleated osteoclasts from mononuclear precursors in murine marrow. J Clin Invest 1995;95:2757–65.

[18] McInnes A, Rennick DM. Interleukin 4 induces cultured monocytes/macrophages to form giant multinucleated cells. J Exp Med 1988;167:598–611.

[19] Meghji S, Morrison MS, Henderson B, Arnett TR. pH dependence of bone resorption: mouse calvarial osteoclasts are activated by acidosis. Am J Physiol: Endocrinol Metab 2001;280:E112–9.

[20] Meuillet EJ, Kroes R, Yamamoto H, Warner TG, Ferrari J, Mania-Farnell B, et al. Sialidase gene transfection enhances epidermal growth factor receptor activity in an epidermoid carcinoma cell line, A431. Cancer Res 1999;59:234–40.

[21] Miyagi T, Wada T, Yamaguchi K, Hata K. Sialidase and malignancy: a minireview. Glycoconj J 2004;20:189–98.

[22] Morishima S, Morita I, Tokushima T, Kawashima H, Miyasaka M, Omura K, et al. Expression and role of mannose receptor/terminal high-mannose type oligosaccharide on osteoclast precursors during osteoclast formation. J Endocrinol 2003;176:285–92.

[23] Moscona A, Peluso RW. Fusion properties of cells persistently infected with human parainfluenza virus type 3: participation of hemagglutinin-neuraminidase in membrane fusion. J Virol 1991;65:2773–7.

[24] Murch AR, Grounds MD, Marshall CA, Papadimitriou JM. Direct evidence that inflammatory multinucleate giant cells form by fusion. J Pathol 1982;137:177–80.

[25] Namba K, Nishio M, Mori K, Miyamoto N, Tsurudome M, Ito M, et al. Involvement of ADAM9 in multinucleated giant cell formation of blood monocytes. Cell Immunol 2001;213:104–13.

[26] Primakoff P, Myles DG. Penetration, adhesion, and fusion in mammalian sperm–egg interaction. Science 2002;296:2183–5.

[27] Schadee-Eestermans IL, Hoefsmit EC, van de Ende M, Crocker PR, van den Berg TK, Dijkstra CD. Ultrastructural localisation of sialoadhesin (siglec-1) on macrophages in rodent lymphoid tissues. Immunobiology 2000;202:309–25.

[28] Semel AC, Seales EC, Singhal A, Eklund EA, Colley KJ, Bellis SL. Hyposialylation of integrins stimulates the activity of myeloid fibronectin receptors. J Biol Chem 2002;277:32830–6.
[29] Stamatos NM, Curreli S, Zella D, Cross AS. Desialylation of glycoconjugates on the surface of monocytes activates the extracellular signal-related kinases ERK 1/2 and results in enhanced production of specific cytokines. J Leukoc Biol 2004;75:307–13.
[30] Stamatos NM, Liang F, Nan X, Landry K, Cross AS, Wang LX, et al. Differential expression of endogenous sialidases of human monocytes during cellular differentiation into macrophages. FEBS J 2005;272: 2545–56.
[31] Suzuki O, Nozawa Y, Abe M. Sialic acids linked to glycoconjugates of Fas regulate the caspase-9-dependent and mitochondria-mediated pathway of Fas-induced apoptosis in Jurkat T cell lymphoma. Int J Oncol 2003;23:769–74.
[32] Suzuki Y, Nagao Y, Kato H, Matsumoto M, Nerome K, Nakajima K, et al. Human influenza A virus hemagglutinin distinguishes sialyloligosaccharides in membrane-associated gangliosides as its receptor which mediates the adsorption and fusion processes of virus infection. Specificity for oligosaccharides and sialic acids and the sequence to which sialic acid is attached. J Biol Chem 1986;261:17057–61.
[33] Tajima M, Higuchi S, Higuchi Y, Miyamoto N, Uchida A, Ito M, et al. Suppression of FRP-1/CD98-mediated multinucleated giant cell and osteoclast formation by an anti-FRP-1/CD98 mAb, HBJ 127, that inhibits c-src expression. Cell Immunol 1999;193: 162–9.
[34] Takeshita S, Kaji K, Kudo A. Identification and characterization of the new osteoclast progenitor with macrophage phenotypes being able to differentiate into mature osteoclasts. J Bone Miner Res 2000;15: 1477–88.
[35] Udagawa N, Takahashi N, Jimi E, Matsuzaki K, Tsurukai T, Itoh K, et al. Osteoblasts/stromal cells stimulate osteoclast activation through expression of osteoclast differentiation factor/RANKL but not macrophage colony-stimulating factor: receptor activator of NF-kappa B ligand. Bone 1999;25:517–23.
[36] Varki A. Sialic acids as ligands in recognition phenomena. FASEB J 1997;11:248–55.
[37] Vignery A. Osteoclasts and giant cells: macrophage–macrophage fusion mechanism. Int J Exp Pathol 2000;81:291–304.
[38] Yagi M, Miyamoto T, Sawatani Y, Iwamoto K, Hosogane N, Fujita N, et al. DC-STAMP is essential for cell–cell fusion in osteoclasts and foreign body giant cells. J Exp Med 2005;202:345–51.

CLINICAL ORTHOPAEDICS AND RELATED RESEARCH
Number 465, pp. 215–219

Factors Affecting Results of Ulnar Shortening for Ulnar Impaction Syndrome

Norimasa Iwasaki, MD, PhD; Jyunichi Ishikawa, MD, PhD*; Hiroyuki Kato, MD, PhD†; Michio Minami, MD, PhD‡; and Akio Minami, MD, PhD**

Although ulnar shortening osteotomy is the most frequently performed operation for ulnar impaction syndrome, little attention has been given to detect certain preoperative factors affecting clinical outcomes of this procedure. We asked whether preoperative factors influenced the postoperative score of ulnar shortening osteotomy combined with arthroscopic débridement of the triangular fibrocartilage complex. We retrospectively reviewed 51 patients (53 wrists) with ulnar impaction syndrome treated with this procedure. There were 28 males and 23 females ranging in age from 14 to 67 years (mean, 37.5 years). The minimum followup was 12 months (mean, 26.3 months; range, 12–95 months). At last followup, we determined a modified Mayo wrist score for each patient. Preoperative factors affecting the clinical score were identified using multiple regression analysis. The clinical score ranged from 40 to 100 points (mean, 84.5 points). A long duration of symptoms and workers' compensation predicted worse clinical scores. We recommend considering these two factors when deciding whether to perform this procedure.

Level of Evidence: Level IV, therapeutic study. See the Guidelines for Authors for a complete description of levels of evidence.

Received: December 5, 2006
Revised: April 27, 2007; August 20, 2007
Accepted: September 7, 2007
From the *Department of Orthopaedic Surgery, Hokkaido University School of Medicine, Sapporo, Japan; the †Department of Orthopaedic Surgery, Shinsyu University School of Medicine, Matsumoto, Japan; and ‡Hokkaido Orthopaedic Memorial Hospital, Sapporo, Japan.
Each author certifies that he or she has no commercial associations (eg, consultancies, stock ownership, equity interest, patent/licensing arrangements, etc) that might pose a conflict of interest in connection with the submitted article.
Each author certifies that his or her institution has approved or waived approval for the human protocol for this investigation and that all investigations were conducted in conformity with ethical principles of research.
Correspondence to: Norimasa Iwasaki, MD, PhD, Department of Orthopaedic Surgery, Hokkaido University School of Medicine, Kita-15, Nishi-7, Kita-Ku, Sapporo 060-8638, Japan. Phone: 81-11-716-1161, ext 5937; Fax: 81-11-706-6054; E-mail: niwasaki@med.hokudai.ac.jp.
DOI: 10.1097/BLO.0b013e31815a9e21

Ulnar impaction syndrome is a complex of symptoms resulting from excessive compression of the ulnar head against the triangular fibrocartilage complex (TFCC) and the ulnar carpal bones. It usually is associated with positive ulnar variance, degenerative changes of the TFCC, ulnocarpal chondromalacia, and lunotriquetral ligament attenuation or tear. These etiologic conditions lead to symptoms, including ulnar wrist pain, limited range of motion of the wrist, and diminished grip strength.

The basis for the surgical treatment of ulnar impaction syndrome reflects an attempt to mechanically decompress the ulnocarpal articulation. Since the first description by Milch,[17] ulnar shortening osteotomy has been a widely accepted procedure for achieving this purpose. Many biomechanical and clinical studies have supported the use of the procedure for ulnar impaction syndrome.[1–5,9,16,21,26–28]

Although ulnar shortening osteotomy is the most frequently performed treatment, numerous authors have reported substantial complications and morbidity associated with this procedure.[2,5,16,20,27] The clinical results of this procedure have varied among previous studies.[2–5,16,20,21,27,28] In terms of this variation, one study indicated patients with specific factors do not respond to ulnar shortening osteotomy.[2] However, little attention has been given to detect certain preoperative factors affecting clinical outcomes of this procedure.

We hypothesized that among 10 preoperative factors, some would influence clinical scores of ulnar shortening osteotomy combined with arthroscopic débridement of the TFCC for ulnar impaction syndrome.

MATERIALS AND METHODS

We retrospectively reviewed the medical records of 51 patients (53 wrists) treated with ulnar shortening osteotomy for ulnar impaction syndrome between March 1993 and March 2005. We included all with the diagnosis who had surgery. We recalled and examined all patients for the last followup, at which time we determined a modified Mayo wrist score[2,6] (modified from

Green and O'Brien[11]) for each patient and the preoperative factors influencing the clinical scores using multiple regression analysis. There were 28 males and 23 females ranging in age from 14 to 67 years (mean, 37.5 years). We performed a power analysis to estimate sample size for determining the least important factors affecting the postoperative clinical score that would be detectable with 80% power with a significance of $\alpha = 0.05$. In a similar study, Iwasaki et al[14] reported a 0.4 correlation coefficient (r) was the least significant value to estimate the predictable factors of radial osteotomies for Kienböck's disease. Using these data and the methods described previously, we ascertained adequate power could be obtained with more than 37 patients.

The dominant hand was involved in 29 patients (58%). All patients presented with ulnar wrist pain of more than 3 months' duration and positive ulnar variance from 1 to 6 mm (mean, 2.8 mm). The duration of symptoms from onset to surgery was 4 to 72 months (mean, 15.3 months). The symptoms were related to occupation in 10 patients, all of whom were covered by workers' compensation. The diagnosis of each patient was made on the basis of treatment history and findings as follows: (1) ulnar wrist pain that was worsened by forearm pronation and ulnar deviation[9]; (2) tenderness just distal to the ulnar head; (3) ulnar wrist pain by axial stress during passive supination-pronation with the wrist in maximum ulnar deviation (positive ulnocarpal stress test)[22]; (4) plain radiographs showing positive ulnar variance with or without cystic changes of the lunate; and (5) arthroscopic findings showing degenerative changes (Class II) of the TFCC according to Palmer's classification.[24] All patients had been treated with nonsteroidal antiinflammatory medications and splinting for more than 3 months. Surgery was performed for patients without responses to these nonoperative treatments. Preexisting distal radioulnar joint (DRUJ) arthritis was considered a contraindication to this procedure. We excluded two patients with bilateral involvement from multiple regression analysis. The minimum followup was 12 months (mean, 26.3 months; range, 12–95 months).

All operations were performed by the senior authors (NI, JI, AM). With the patients under general anesthesia with a tourniquet, arthroscopic procedures were performed according to a method described previously.[18,30] The lunotriquetral interosseous ligaments and the TFCC were inspected for wear or tear. The articular surfaces of the lunate and the triquetrum also were examined. In all patients, débridement of the TFCC wear or tear to a stable margin was performed using a small joint cutter (2.5-mm diameter; Stryker Corp, San Jose, CA) or an electrothermal small joint probe (Vulcan® EAS; Smith and Nephew, Inc, Andover, MA). After arthroscopic procedures, ulnar shortening osteotomy was performed. The distal ulna was approached through a longitudinal incision between the extensor carpi ulnaris and the flexor carpi ulnaris. The dorsal sensory branch of the ulnar nerve was protected and the distal ulna was exposed subperiosteally. A six-hole small dynamic compression plate was placed on the surface of the ulna as distal as possible. The three most proximal screw holes then were drilled and the screws were inserted to determine the osteotomy site. Only the most proximal screw remained and the plate was swung away from the osteotomy site. Parallel transverse osteotomies were performed to remove an appropriate segment of the bone. The length of the removed segment equaled the amount of positive ulnar variance measured on the preoperative radiograph (Fig 1A). The plate was swung back in place and the two proximal screws were reinserted. The remaining distal screws were introduced in the compression mode (Fig 1B). Postoperatively, a below-elbow splint was applied for 2 weeks. Active and passive motion of the wrist was started after the splint was removed.

As described above, we (NI, MM) determined the modified Mayo wrist score for each patient at followup. Ten preoperative patient factors as independent variables were obtained from the medical record of each patient (Table 1). We (NI, MM) measured perioperative ulnar variances radiographically using the method of perpendiculars whereby a line is drawn perpendicular to the longitudinal axis of the radius at its distal ulnar aspect and the distance between it and the line at the end of the ulna is measured.[10,12] For accurate determination of ulnar variance, a posteroanterior radiograph of the wrist was obtained with the shoulder in 90° abduction, the elbow in 90° flexion, the forearm in neutral rotation, and the wrist in neutral alignment.[25] One of us (NI, blinded to the clinical score) evaluated the radiographs. Degenerative changes of the DRUJ were noted, including osteophytes on the inferior edge of the DRUJ, joint space narrowing, and subchondral sclerosis.[12] Intraobserver variation in the measurement of ulnar variance was assessed by calculating the coefficient of variation, which equals the standard deviation divided by the mean value. The observer performed five measurements of ulnar variance in the same radiograph. The coefficient of variation among the results of five sets was calculated. The value was 9%, suggesting high reliability of the radiographic measurement for one individual.

Preoperative factors affecting the clinical score were detected using multiple regression analysis. This analysis focused on the

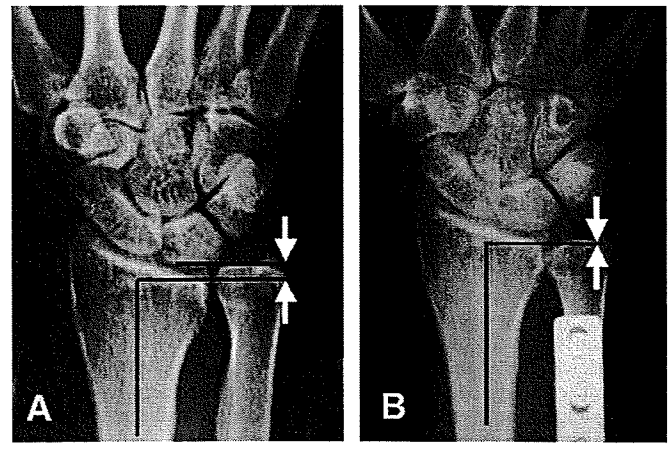

Fig 1A–B. (A) The length of the removed segment equals the amount of positive ulnar variance (arrows) measured on the posteroanterior radiograph. (B) Zero ulnar variance is achieved after ulnar shortening osteotomy and fixation with a six-hole small dynamic compression plate. Joint space narrowing of the DRUJ is found at 16 months postoperatively.

TABLE 1. List of Variables Used in Multiple Regression Analysis

Variable	Type of Variable
Dependent	
Postoperative clinical score	C
Independent	
Patient age	C
Affected side	NC
Workers' compensation	NC
Pain	NC
Symptom duration	C
Preoperative range of motion of the wrist	C
Preoperative grip strength (percentage of unaffected side)	C
Preoperative clinical score	C
Palmer's arthroscopic classification of triangular fibrocartilage complex lesions[24]	NC
Ulnar shortening amount	C

C = continuous variable; NC = noncontinuous variable

wrist score as a dependent variable and the preoperative factors as independent variables. Paired t tests were conducted to analyze differences in clinical scores and radiographic measurements before and after surgery. All analyses were performed using commercial software (StatView®; SAS Institute Inc, Cary, NC). The obtained data were expressed as mean ± standard deviation. The level of significance was set at $p < 0.05$.

RESULTS

Arthroscopy showed degeneration of the TFCC and chondromalacia of the lunate in all patients. A central perforation was seen in 37 of the 53 wrists (70%). According to Palmer's classification of TFCC lesions, Class IIB lesions were present in 16 wrists (30%), Class IIC in nine (17%), Class IID in 25 (48%), and Class IIE in three (5%). Bony union at the site of the osteotomy was achieved within 16 weeks in all patients except one. The remaining patient achieved bony union at 24 weeks without any surgery. The mean postoperative ulnar variance decreased ($p < 0.0001$) from 2.8 ± 1.1 mm to 0.5 ± 1.0 mm. The mean postoperative value at followup improved ($p < 0.0001$) compared with the preoperative value (Table 2). Thirty (56%) wrists were free from pain and 18 (35%) had occasional pain. The remaining five (9%) wrists had moderate pain without improvement postoperatively. The mean subjective pain score at followup improved ($p < 0.0001$) compared with the preoperative value (Table 2). The mean postoperative range of extension and flexion of the wrist increased ($p < 0.005$), whereas that of pronation and supination of the forearm did not considerably alter (Table 2). The postoperative grip strength of the affected side was similar to that

TABLE 2. Preoperative and Postoperative Clinical Outcomes

Criteria	Preoperative	Postoperative
Pain score	6.8 ± 5.2	22.0 ± 4.6*
Range of wrist motion (flexion-extension arc)	144.6° ± 28.8°	155.8° ± 25.1°†
Range of forearm motion (pronation-supination arc)	164.8° ± 14.7°	165.5° ± 11.3°
Grip strength (percentage of unaffected side)	83.5% ± 27.2%	91.1% ± 26.1%
Functional status score	10.2 ± 7.1	20.2 ± 6.6*
Overall clinical score	52.1 ± 13.1	84.5 ± 16.4*

Values are expressed as mean ± standard deviation; *$p < 0.0001$; †$p < 0.005$

of the unaffected side (Table 2). Twenty-nine (57%) of the patients returned to the same activities and 19 (38%) had restrictions to their activities. These patients returned to their original sport or job. Three patients changed vocation or sport. The functional score increased ($p < 0.0001$) at followup.

The duration of symptoms and workers' compensation influenced postoperative clinical scores (Table 3): a long duration of symptoms and workers' compensation negatively predicted the clinical score after ulnar shortening osteotomy. Preoperative symptoms for greater than 6 months predicted lower ($p < 0.005$) postoperative clinical scores (74.1 ± 21.3 versus 88.3 ± 12.0). Patients receiving workers' compensation had the likelihood of lower ($p < 0.0005$) clinical scores (68.3 ± 18.5 versus 88.9 ± 12.8).

Twenty-nine wrists (55%) experienced hardware irritation. For these patients, the hardware was removed at a mean of 22.5 months (range, 7–95 months) after surgery. There were no other serious postoperative complications.

TABLE 3. Results of Multiple Regression Analysis

Independent Variable	Coefficient	p Value
Patient age	−0.047	NS
Affected side	0.136	NS
Workers' compensation	−0.432	0.036
Pain	−0.046	NS
Symptom duration	0.421	0.043
Preoperative range of motion of the wrist	0.345	NS
Preoperative grip strength (percentage of unaffected side)	0.317	NS
Preoperative clinical score	0.425	NS
Palmer's arthroscopic classification of triangular fibrocartilage complex lesions[24]	0.048	NS
Ulnar shortening amount	0.028	NS

NS = no significance

Radiographically, an osteophyte on the inferior edge of the joint was seen in 12 (23%) of 53 wrists. Joint space narrowing and subchondral sclerosis were observed in eight (15%) wrists and one (2%) wrist, respectively. In 13 (34%) wrists, there were some postoperative degenerative changes at the DRUJ. However, there were no substantial differences in the clinical scores between patients without and with postoperative degenerative changes of the DRUJ (85.2 ± 14.9 versus 81.1 ± 19.0).

DISCUSSION

Although ulnar shortening osteotomy is the most frequently performed operation for ulnar impaction syndrome, the clinical results of this procedure have varied.[2–5,16,20,21,27,28] One of the reasons for these variations may be that patients with some specific factors do not respond to ulnar shortening osteotomy.[2] Another reason is that most of the outcomes have been based on a small number of patients.[2–5,16,21,28] To date, there have been no statistical analyses to detect certain preoperative factors affecting clinical outcomes of this procedure. In this study, we obtained the postoperative clinical scores of ulnar shortening osteotomy combined with arthroscopic débridement of the TFCC for ulnar impaction syndrome and then determined which preoperative factors affected the scores.

Our study has several limitations. First, our analysis was based on data from retrospective chart review. To confirm the predictable effects of each factor obtained here, a prospective and controlled design is required to ensure the preoperative data are collected in a standard fashion. Second, because of the relatively short followup (minimum, 12 months; mean, 26 months), degenerative changes of the DRUJ would not likely have fully developed and thus might not have influenced the clinical results as they might in the future. A longer followup in such cohorts is needed to confirm our results.

Our data suggest this procedure for ulnar impaction syndrome improved the modified Mayo wrist score from 52 to 84 points. The variation in this score suggests the outcomes of ulnar shortening osteotomy combined with arthroscopic débridement of the TFCC for treatment of ulnar impaction syndrome vary more than we expected. Therefore, we should consider whether a patient with ulnar impaction syndrome is an ideal candidate for this procedure.

Elucidation of preoperative factors affecting clinical results after ulnar shortening osteotomy is useful to select appropriate patients for this procedure. The duration of symptoms and workers' compensation were the two factors affecting the clinical scores—more than 6 months' persistence of symptoms and workers' compensation were substantial negative predictors of clinical outcomes after this procedure. The main causes of inferior clinical outcomes in patients receiving workers' compensation and a long persistence of symptoms cannot be statistically proven. However, in patients receiving workers' compensation, some social factors or high physical demands on the surgically treated wrist seem to be the main causes. The patients with a long persistence of symptoms may be attributable to the severity of clinical symptoms and to pathologic changes in the wrist. Our data indicate patients receiving workers' compensation with more than 6 months' duration of symptoms may not respond favorably to this procedure.

Some investigators have reported variable clinical outcomes after ulnar shortening osteotomy for ulnar impaction syndrome (Table 4). Reasons for the variability include small numbers of patients, variable followup times, and use of two outcome instruments. Therefore, a larger population study, including patients with affecting factors, is required to achieve reliable postoperative outcomes of this procedure. We believe the larger number of patients in our study provides more reliable information for this procedure.

A consideration after performing ulnar shortening osteotomy is its mechanical effects on the DRUJ. Nishiwaki et al,[23] using a cadaveric model, showed the stiffness of the DRUJ substantially increased after ulnar shortening of 3 to 6 mm. Deshmukh et al[7] reported that after 2-mm shortening of the ulna, the joint contact area of the DRUJ decreased in cadaveric wrist specimens. In addition, the area of contact moved proximally on the sigmoid notch of the radius. We interpret these mechanical effects on the DRUJ as increasing the risk of osteoarthritic changes after ulnar shortening. In this study, postoperative osteoarthritic

TABLE 4. Clinical Outcomes after Ulnar Shortening Osteotomy for Ulnar Impaction Syndrome

Study (year)	Number of Wrists	Mean Followup (months)	Percent Good or Excellent (assessment system)
Chun and Palmer[4] (1993)	30	51	93% (modified Gartland-Werley[4])
Fricker et al[8] (1996)	28	20	43% (modified Gartland-Werley[4])
Nagle and Bernstein[21] (2002)	11	31	82% (modified Mayo[2,6])
Bernstein et al[2] (2004)	16	15	69% (modified Mayo[2,6])
Baek et al[1] (2005)	31	32	94% (modified Gartland-Werley[4])
Current study (2007)	53	26	66% (modified Mayo[2,6])

changes of the DRUJ were seen in 34% of wrists. Previous clinical studies also showed 20% to 40% of patients treated with this procedure exhibited radiographic evidence of DRUJ osteoarthritis after 2 to 3 years.[7,15,19] Our data confirm these results. However, we found no relationship between such radiographic changes and clinical results.

We have provided the outcomes of combined arthroscopic TFCC débridement and ulnar shortening osteotomy for ulnar impaction syndrome. The data make us question whether arthroscopic TFCC débridement is required for improving clinical outcomes for this disease. Bernstein et al[2] reported combined arthroscopic TFCC débridement and ulnar shortening osteotomy provided satisfactory results for patients with ulnar impaction syndrome. However, Baek et al[1] reported ulnar shortening alone performed in patients with idiopathic ulnar impaction syndrome resulted in considerable improvement in wrist symptoms and functions. Minami et al[18] reported arthroscopic débridement of the TFCC provided fair or poor results for patients with degenerative TFCC tears and ulnar impaction syndrome. Other investigators also have stated débridement alone is unsuccessful in wrists with positive ulnar variance.[13,29] Therefore, we believe the improvement in clinical outcomes results mainly from surgical effects of ulnar shortening osteotomy alone.

Ulnar shortening osteotomy combined with arthroscopic débridement of the TFCC is effective for treating ulnar impaction syndrome. Our data indicate there is lower effectiveness of ulnar shortening osteotomy when performing this procedure for patients receiving workers' compensation with a long duration of symptoms.

Acknowledgment

We thank Dr. Yasuhiko Nishio for the data collection of the patients.

References

1. Baek GH, Chung MS, Lee YH, Gong HS, Lee S, Kim HH. Ulnar shortening osteotomy in idiopathic ulnar impaction syndrome. *J Bone Joint Surg Am.* 2005;87:2649–2654.
2. Bernstein MA, Nagle DJ, Martinez A, Stogin JM Jr, Wiedrich TA. A comparison of combined arthroscopic triangular fibrocartilage complex debridement and arthroscopic wafer distal ulna resection versus arthroscopic triangular fibrocartilage complex debridement and ulnar shortening osteotomy for ulnocarpal abutment syndrome. *Arthroscopy.* 2004;20:392–401.
3. Boulas HJ, Milek MA. Ulnar shortening for tears of the triangular fibrocartilaginous complex. *J Hand Surg Am.* 1990;15:415–420.
4. Chun S, Palmer AK. The ulnar impaction syndrome: follow-up of ulnar shortening osteotomy. *J Hand Surg Am.* 1993;18:46–53.
5. Constantine KJ, Tomaino MM, Herndon JH, Sotereanos DG. Comparison of ulnar shortening osteotomy and the wafer resection procedure as treatment for ulnar impaction syndrome. *J Hand Surg Am.* 2000;25:55–60.
6. Cooney WP, Linscheid RL, Dobyns JH. Triangular fibrocartilage tears. *J Hand Surg Am.* 1994;19:143–154.
7. Deshmukh SC, Shanahan D, Coulthard D. Distal radioulnar joint incongruity after shortening of the ulna. *J Hand Surg Br.* 2000;25:434–438.
8. Fricker R, Pfeiffer KM, Troeger H. Ulnar shortening osteotomy in posttraumatic ulnar impaction syndrome. *Arch Orthop Trauma Surg.* 1996;115:158–161.
9. Friedman SL, Palmer AK. The ulnar impaction syndrome. *Hand Clin.* 1991;7:295–310.
10. Gelberman R, Salamon P, Jurist JM, Posch JL. Ulnar variance in Kienböck's disease. *J Bone Joint Surg Am.* 1975;57:674–676.
11. Green DP, O'Brien ET. Open reduction of carpal dislocations: indications and operative techniques. *J Hand Surg Am.* 1978;3:250–265.
12. Hollevoet N, Verdonk R, Van Maele G. The influence of articular morphology on non-traumatic degenerative changes of the distal radioulnar joint: a radiographic study. *J Hand Surg Br.* 2006;31:221–225.
13. Hulsizer D, Weiss AP, Akelman E. Ulnar-shortening osteotomy after failed arthroscopic debridement of the triangular fibrocartilage complex. *J Hand Surg Am.* 1997;22:694–698.
14. Iwasaki N, Minami A, Oizumi N, Yamane S, Suenaga N, Kato H. Predictors of clinical results of radial osteotomies for Kienböck's disease. *Clin Orthop Relat Res.* 2003;415:157–162.
15. Koppel M, Hargreaves IC, Herbert TJ. Ulnar shortening osteotomy for ulnar carpal instability and ulnar carpal impaction. *J Hand Surg Br.* 1997;22:451–456.
16. Loh YC, Van Den Abbeele K, Stanley JK, Trail IA. The results of ulnar shortening for ulnar impaction syndrome. *J Hand Surg Br.* 1999;24:316–320.
17. Milch H. Cuff resection of the ulna for malunited Colles' fracture. *J Bone Joint Surg.* 1941;23:311–313.
18. Minami A, Ishikawa J, Suenaga N, Kasashima T. Clinical results of treatment of triangular fibrocartilage complex tears by arthroscopic debridement. *J Hand Surg Am.* 1996;21:406–411.
19. Minami A, Kato H. Ulnar shortening for triangular fibrocartilage complex tears associated with ulnar positive variance. *J Hand Surg Am.* 1998;23:904–908.
20. Moholkar K, Smyth H. Acute compartment syndrome of the forearm in association with ulnar shortening osteotomy: a case report. *J Hand Surg Am.* 2000;25:358–359.
21. Nagle DJ, Bernstein MA. Laser-assisted arthroscopic ulnar shortening. *Arthroscopy.* 2002;18:1046–1051.
22. Nakamura R, Horii E, Imaeda T, Nakao E, Kato H, Watanabe K. The ulnocarpal stress test in the diagnosis of ulnar-sided wrist pain. *J Hand Surg Br.* 1997;22:719–723.
23. Nishiwaki M, Nakamura T, Nakao Y, Nagura T, Toyama Y. Ulnar shortening effect on distal radioulnar joint stability: a biomechanical study. *J Hand Surg Am.* 2005;30:719–726.
24. Palmer AK. Triangular fibrocartilage complex lesions: a classification. *J Hand Surg Am.* 1989;14:594–606.
25. Palmer AK, Glisson RR, Werner FW. Ulnar variance determination. *J Hand Surg Am.* 1982;7:376–379.
26. Palmer AK, Werner FW. Biomechanics of the distal radioulnar joint. *Clin Orthop Relat Res.* 1984;187:26–35.
27. Sunil TM, Wolff TW, Scheker LR, McCabe SJ, Gupta A. A comparative study of ulnar-shortening osteotomy by the freehand technique versus the Rayhack technique. *J Hand Surg Am.* 2006;31:252–257.
28. Tatebe M, Nakamura R, Horii E, Nakao E. Results of ulnar shortening osteotomy for ulnocarpal impaction syndrome in wrists with neutral or negative ulnar variance. *J Hand Surg Br.* 2005;30:129–132.
29. Tomaino MM, Weiser RW. Combined arthroscopic TFCC debridement and wafer resection of the distal ulna in wrists with triangular fibrocartilage complex tears and positive ulnar variance. *J Hand Surg Am.* 2001;26:1047–1052.
30. Whipple TL. *The Wrist.* Philadelphia, PA: JB Lippincott Co; 1992.

Osteoarthritis and Cartilage (2008) **16,** 772–778

doi:10.1016/j.joca.2007.11.004

Osteoarthritis and Cartilage

International Cartilage Repair Society

OARSI OSTEOARTHRITIS RESEARCH SOCIETY INTERNATIONAL

Alteration of *N*-glycans related to articular cartilage deterioration after anterior cruciate ligament transection in rabbits[1]

T. Matsuhashi M.D.†, N. Iwasaki M.D., Ph.D., Associate Professor†*, H. Nakagawa Ph.D., Associate Professor‡, M. Hato‡, M. Kurogochi Ph.D.‡, T. Majima M.D., Ph.D., Associate Professor†, A. Minami M.D., Ph.D., Professor† and S.-I. Nishimura Ph.D., Professor‡

† *Department of Orthopaedic Surgery, Hokkaido University Graduate School of Medicine, Sapporo, Japan*

‡ *Graduate School of Advanced Life Science, Frontier Research Center for Post-Genome Science and Technology, Hokkaido University, Sapporo, Japan*

Summary

Objective: Osteoarthritis (OA) is the most common of all joint diseases, but the molecular basis of its onset and progression is controversial. Several studies have shown that modifications of *N*-glycans contribute to pathogenesis. However, little attention has been paid to *N*-glycan modifications seen in articular cartilage. The goal of this study was to identify disease specific *N*-glycan expression profiles in degenerated cartilage in a rabbit OA model induced by anterior cruciate ligament transection (ACLT).

Methods: Cartilage samples were harvested at 7, 10, 14, and 28 days after ACLT and assessed for cartilage degeneration and alteration in *N*-glycans. *N*-Glycans from cartilage were analyzed by high performance liquid chromatography and mass spectrometry.

Results: Histological analysis showed that osteoarthritic changes in cartilage occurred 10 days after ACLT. Apparent alterations in the *N*-glycan peak pattern in cartilage samples were observed 7 days after ACLT, and overall *N*-glycan changes in OA reflected alterations in both sialylation and fucosylation. These changes apparently preceded histological changes in cartilage.

Conclusion: These results indicate that changes in the expression of *N*-glycans are correlated with OA in an animal model. Understanding mechanisms underlying changes in *N*-glycans seen in OA may be of therapeutic value in treating cartilage deterioration.

Key words: Cartilage, Osteoarthritis, *N*-Glycan.

Introduction

Chondrocyte metabolism is controlled by genetic and environmental factors, such as extracellular matrix (ECM) composition, soluble mediators, or mechanical factors[1,2]. Osteoarthritis (OA), which results from a breakdown in the balance of these factors, is the most common joint disease. To date, numerous studies have investigated its pathogenesis[1–8]. However, factors mediating onset and aggravation of OA are still controversial.

Glycobiology, defined as the analysis of biological function of sugar chains covalently bound to proteins and lipids, has been recently applied to molecular-based investigations[9]. Sugar chains attached to proteins (glycoproteins) and lipids (glycolipids) are commonly referred to as glycans. Glycoprotein glycans are found on the cell surface, in the ECM, and in serum. These glycans act as an interface on the cell surface and modulate protein properties, including folding, secretion, targeting, and protease resistance[10,11]. Several studies show that glycan modifications of proteins contribute to the pathogenesis of some diseases[12,13]. One characteristic of cartilage is that some chondrocytes reside in areas rich in ECM. In addition, it is well known that glycoproteins are abundant on the cell surface and in cartilage ECM. These observations lead to a working hypothesis that sugars attached to proteins contribute to chondrocyte metabolism.

Glycans attached to proteins are classified into two groups: glycans attached to an asparagine residue through a nitrogen atom (*N*-glycans) and those attached to a serine or threonine oxygen (*O*-glycans)[11]. Both types have been intensively studied, and many studies report structural and functional analyses of *N*-glycans[14]. Based on these data, a relationship between *N*-glycan alteration and disease has recently been emerged[12,13,15–18]. For example, several studies of *N*-glycans of serum immunoglobulin G (IgG) molecules associated with the rheumatoid arthritis (RA) indicate that changing *N*-glycan structure contributes to RA[19–21]. However, little attention has been paid to *N*-glycan alterations occurring in articular cartilage in a diseased condition.

Glycans have five major functions: (1) providing cell wall and ECM structural components, (2) modifying protein

[1]Supported by a grant for the National Project on "Functional Glycoconjugate Research Aimed at Developing New Industry" from the Ministry of Education, Science, Sport and Culture of Japan, and SENTAN from the Japan Science and Technology Agency and Uehara Memorial Foundation.

*Address correspondence and reprint requests to: Dr Norimasa Iwasaki, Department of Orthopaedic Surgery, Hokkaido University Graduate School of Medicine, 060-8638, North 15, West 7, Kita-ku, Sapporo, Hokkaido, Japan. Tel: 81-11-706-5936 ext. 5937; Fax: 81-11-706-6054; E-mail: niwasaki@med.hokudai.ac.jp

Received 11 November 2006; revision accepted 17 November 2007.

properties, (3) directing glycoconjugates, (4) mediating and modulating cell adhesion, and (5) mediating and modulating signaling. Thus, we hypothesized that cartilage *N*-glycans would be altered in parallel with cartilage degradation in OA and would vary according to the degree of deterioration. Particularly, *N*-glycan alterations should occur at early phases of OA aggravation. To test this hypothesis, we analyzed *N*-Glycans of rabbit OA cartilage explants induced by anterior cruciate ligament transection (ACLT). The specific aims of this study were to clarify the alterations in cartilage *N*-glycans with OA aggravation and to identify *N*-glycan structures correlated with cartilage deterioration.

Materials and methods

ANIMALS AND SURGICAL PROCEDURES

Seventy-eight adult female Japanese white rabbits (15–16-week-old) weighing 2.6–3.1 kg purchased from a professional breeder (Japan SLC, Inc., Hamamatsu, Japan) were used for this study according to the established ethical guidelines approved by the local animal care committee. Rabbits were anesthetized with 0.6 ml pentobarbital sodium (50 mg/ml) injections and then maintained on isoflurane. To induce osteoarthritic changes of articular cartilage, the right knee ACL was sectioned through a medial parapatellar incision (OA group). As a sham control, arthrotomy without ACLT was performed in sham group. Rabbits were housed in plastic cages and allowed to move freely after the operation. At days 0, 7, 10, 14, and 28, animals were euthanized by an intravenous injection of overdose pentobarbital to obtain cartilage samples for histological and glycostructural analyses. Serum samples were harvested prior to euthanasia. Here, day 7 is defined as 7 days after the operation, and day 0 means the day prior to the operation.

HISTOLOGICAL ANALYSIS ($N = 36$)

To determine osteoarthritic changes in OA and sham groups, cartilage samples ($n = 4$) were analyzed histologically at days 0, 7, 10, 14, and 28. Each sample, including the tibial plateau and femoral condyle, was fixed in 10% neutral buffered formalin. Tissue blocks were decalcified with 14% ethylenediaminetetraacetic acid (EDTA), cut in a sagittal plane, and stained with hematoxylin and eosin (HE) and Safranin O–fast green. To avoid observer bias, slides were coded prior to microscopic analysis. Osteoarthritic changes in each sample were quantified using the modified Mankin score[22].

PREPARATION OF PYRIDYLAMINATED (PA)-*N*-GLYCAN ($N = 42$)

Cartilage samples of the tibial plateau and serum were obtained from each animal at days 0, 7, 10, and 28. Cartilage minced by a razor and serum was heated to 90°C for 15 min. After lyophilization, each sample was digested sequentially with trypsin, chymotrypsin, *N*-glycosidase F, and pronase as described[23]. *N*-Glycan fractions were purified on a gel-filtration column (Bio-Gel P-4, 1 × 38 cm, water, Nippon Bio-Rad Laboratories KK, Tokyo, Japan), and tagged by fluorescent labeling using 2-aminopyridine to increase sensitivity for analysis[24]. Excess reagents were removed by gel-filtration on Sephadex-G-15 (Amersham Bioscience, Tokyo, Japan). PA-*N*-glycans were analyzed using high performance liquid chromatography (HPLC) and mass spectrometry (MS).

HPLC ANALYSIS

HPLC analysis using the L-7000 HPLC system (Hitachi High-Technologies, Tokyo, Japan) was performed under conditions previously described[25,34,36]. PA-*N*-glycans were separated on an octadecylsilica (ODS) column (HRC-ODS, 6 × 150 mm, Shimadzu, Kyoto, Japan), and each peak on the ODS column was applied individually to an amide column (TSK-gel Amide-80, 4.6 × 250 mm, Tosoh, Tokyo, Japan). The relative amount of PA-*N*-glycans was calculated based on the peak area analyzed by attached software on the HPLC system. Elution positions of PA-*N*-glycan on the ODS and amide columns were converted to glucose units (GU), which corresponded to relative degree of polymerization of α1,6-glucose oligosaccharides, for increasing reproducibility. *N*-Glycan structures were suggested by comparing elution positions with data reported in the same analytical conditions, and confirmed with further HPLC analysis combined with partial digestion, and/or MS. Elution positions and code numbers of approximately 500 kinds of oligosaccharide are described in these references[34,35]. The validity of the elution positions and partial digestions was confirmed using well-known standard PA-*N*-glycans and previous studies[27,36].

N-Glycans can form various structures, but have a common core structure and some rules in linkages[11]. To determine the detailed *N*-glycans' structure related to OA, PA-*N*-glycans were digested sequentially with β-*N*-acetylhexosaminidase (HexNAcase, Jack bean, Seikagaku Co., Tokyo, Japan) which removed β-linked GalNAc and GlcNAc, α1,3/4-fucosidase (α3/4-Fase, Takara Co., Shiga, Japan) and weak hydrochloric acid to hydrolyze sialic acids. After each digestion, PA-*N*-glycans were individually analyzed by HPLC on both columns to confirm elution positions[23,25].

MS

To identify the PA-*N*-glycan structure, some PA-*N*-glycans separated by HPLC were further analyzed by matrix-assisted laser desorption/ionization time-of-flight MS (MALDI-TOF MS) using an Ultraflex TOF/TOF mass spectrometer (Bruker Daltonics GmbH, Bremen, Germany). As matrices, 2,5-dehydroxybenzoic acid (DHB) and α-cyano-4-hydroxycinnaminic acid (CHCA) were used. PA-*N*-glycans fractionated on HPLC were dissolved and applied to MALDI-TOF MS as described[26]. Based on results from HPLC and MS, each precise *N*-glycan structure was determined.

All measurements were performed using an Ultraflex TOF/TOF mass spectrometer equipped with a reflector and controlled by the FlexControl 2.2 software package (Bruker Daltonics). In MALDI-TOF MS reflector mode, ions generated by a pulsed UV laser beam (nitrogen laser, $\lambda = 337$ nm, 5 Hz) were accelerated to a kinetic energy of 23.5 kV. Metastable ions generated by laser-induced decomposition of the selected precursor ions were analyzed without any additional collision gas. In MALDI-LIFT-TOF/TOF mode, precursor ions were accelerated to 8 kV and selected in a timed ion gate. The fragments were further accelerated by 19 kV in the LIFT cell (LIFT indicates "lifting" the potential energy for the second acceleration of ion source), and their masses were analyzed after the ion reflector passage. Masses were automatically annotated by using the FlexAnalysis 2.2 software package. External calibration of MALDI mass spectra was carried out using singly charged monoisotopic peaks of a peptide mixture of human angiotensin II (*m/z* 1046.542), bombesin (*m/z* 1619.823), ACTH-(18–39) (*m/z* 2465.199), and somatostatin 28 (*m/z* 3147.472).

STATISTICAL ANALYSIS

Data were represented as means ± standard deviation (SD). Significant differences between groups were assessed by unpaired *t* tests. *P*-values of less than 0.05 were considered significant.

Results

HISTOLOGICAL FINDINGS

After the operations, rabbits exhibited a normal gait pattern by footprint analysis (data not shown). Also, infections were not seen macroscopically in any knee joint (data not shown). At day 7, no histological changes of the tibial plateau were seen in HE-stained samples of the OA group [Fig. 1(b)]. Samples evaluated at day 10 showed common OA changes, including deterioration of the superficial cartilage layer and a reduced number of chondrocytes in superficial and middle cartilage layers [Fig. 1(c)]. At day 28, a reduced number of chondrocytes were observed in whole layers [Fig. 1(e)], and cloning of chondrocytes was apparent in these damaged areas [Fig. 1(e)]. While Safranin O–fast green staining showed no significant change from day 7 to day 14 [Fig. 1(g–i)], both showed significant reduction at day 28 [Fig. 1(j)]. In the sham group, from day 7 to day 28 no histological indications of OA changes were observed in any samples (data not shown). Histological changes of the femoral condyle were observed later than histological changes of the tibial plateau (data not shown). After day 10, mean histological scores of the tibial plateau were significantly higher in the OA group than in the sham group (3.6 ± 0.5 vs 2.3 ± 0.5 at day 10, $P < 0.05$; 7.0 ± 0.6 vs 2.4 ± 0.4 at day 28, $P < 0.05$, Fig. 2).

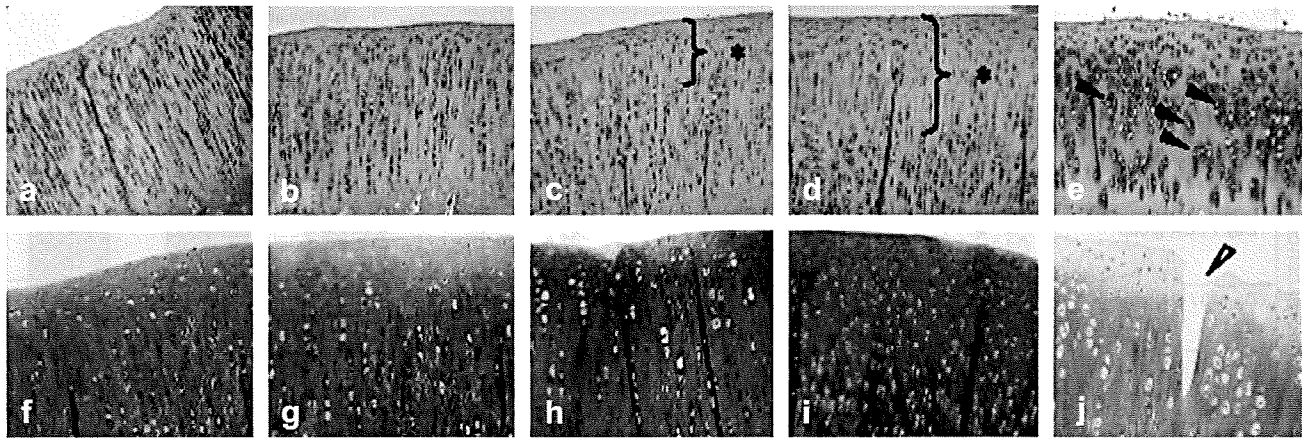

Fig. 1. Histology of cartilage after ACLT in medial tibial plateau in the rabbit knee joint. (a–e) HE-stained sections. (f–j) Safranin O-fast green stained sections. (a) Control articular cartilage shows a smooth surface. (b) At day 7, no significant changes compared with control cartilage were observed. (c) At day 10, superficial diffuse loss of chondrocytes (*) with surface irregularity was observed. (d) At day 14, diffuse loss of chondrocytes from superficial and middle zones (*) with surface irregularity was observed. (e) At day 28, diffuse loss of chondrocytes in the whole zone with clone formation (solid arrow) was observed. (f) Control articular cartilage with Safranin O-fast green stain. (g–i) At days 7,10, and14, no significant change of Safranin O-fast green staining was observed. (j) At day 28, severe loss of Safranin O–fast green staining and clefts (empty arrow) was observed.

ALTERATION IN *N*-GLYCAN PROFILES

We found no significant alterations in the *N*-glycan peak pattern of serum from day 7 to day 28 in the OA group (Fig. 3). In cartilage analysis, there were no apparent alterations in the *N*-glycan peak pattern from day 7 to day 28 in the sham group. By contrast, significant alterations in the *N*-glycan peak pattern in cartilage were observed in the OA group from day 7 postoperatively (Fig. 4). Alterations in peak shape suggested a change in the composition of *N*-glycans contained in the peak. To confirm this, we purified peaks by HPLC on an ODS column and analyzed each on an amide column in a different chromatographic mode. Each altered peak on the ODS column was separated into three peaks on the amide column, referred to as *N*-glycan A (a), B (b), and C (c) in the order of separation time (Fig. 4*). We then calculated each area ratio. The mean ratio of *N*-glycan A in the OA group significantly decreased from day 7 to day 28 compared to the sham group (40.6 ± 1.80 vs 36.0 ± 1.40 at day 7, $P < 0.05$; 39.8 ± 1.54 vs 35.6 ± 1.97 at day 28, $P < 0.05$, Fig. 5), while the value of *N*-glycan C in the OA group significantly increased from day 7 compared to the sham group (44.7 ± 1.91 vs 40.8 ± 1.28 at day 7, $P < 0.05$; 46.0 ± 2.67 vs 40.2 ± 1.03 at day 28, $P < 0.05$, Fig. 5). The mean ratio of *N*-glycan B did not significantly change (data not shown). The mean ratio of *N*-glycans A–C after day 7 was significantly higher in the OA group than in the sham group (1.25 ± 0.11 vs 1.01 ± 0.04 at day 7, $P < 0.05$; 1.32 ± 0.11 vs 1.01 ± 0.04 at day 28, $P < 0.05$, Fig. 5).

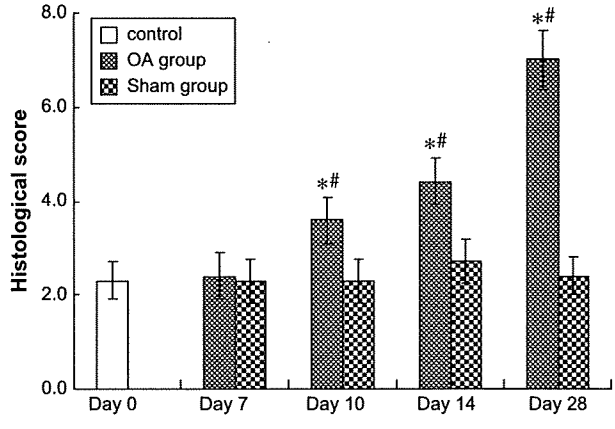

Fig. 2. Histological scores of medial tibial plateau. Values are means ± SD. Shown are scores for histological parameters with comparisons between groups. Histological analysis revealed that slightly degenerative changes in cartilage occurred in all cases starting 10 days after ACLT. *Denotes statistical significance ($P < 0.05$) vs sham group. #Denotes statistical significance ($P < 0.05$) vs control.

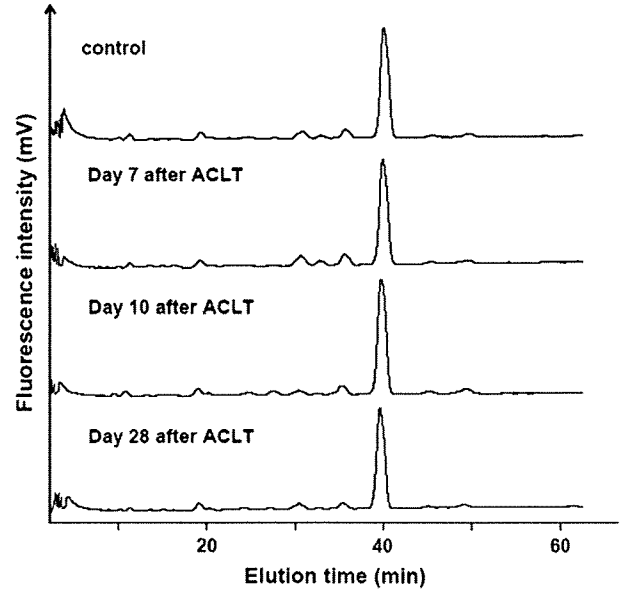

Fig. 3. Chromatograms of PA-*N*-glycans obtained from rabbit serum glycoproteins on an ODS column. There were no significant alterations in the *N*-glycan peak pattern of serum from day 7 to day 28 in the OA group compared with controls.

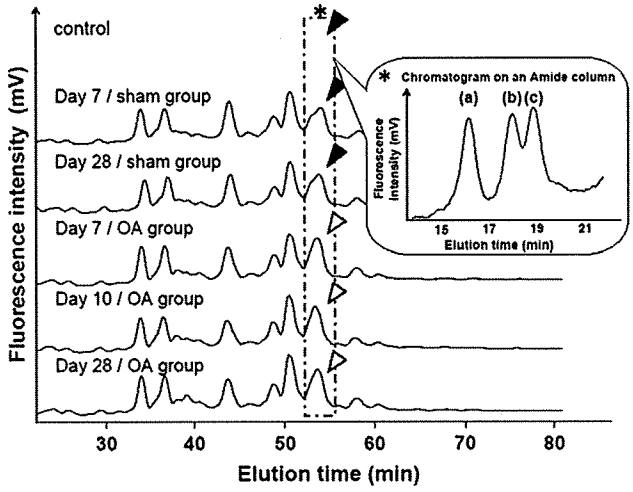

Fig. 4. Chromatograms of PA-*N*-glycans obtained from rabbit cartilage glycoproteins on an ODS column. Two peaks (solid arrow) in the chart of day 0 and the sham-operated group were seen as one peak (empty arrow) from day 7 after ACLT. Those peaks included three peaks on an amide column, referred to as *N*-glycan A (a), B (b), and C (c), in the order of separation time (*).

STRUCTURAL ANALYSIS OF *N*-GLYCANS RELATED TO OSTEOARTHRITIC CHANGES

MALDI-TOF spectra of *N*-glycans A and C with DHB as a matrix indicated a molecular mass of 2239.6 and 2094.6, respectively (Fig. 6). Each MALDI-TOF/TOF spectra showed constituents of *N*-glycans A and C (Fig. 7). MALDI-TOF and TOF/TOF spectra of *N*-glycans with CHCA as a different matrix indicated almost the same mass fragmentation compared with DHB (data not shown). Molecular mass of 2239.6 and 2094.6 corresponds with a protonated PA-glycan which consists of 3 Hex, 6 HexNAc and *N*-acetylneuraminic acid (NANA); and 3 Hex, 6 HexNAc and Fuc, respectively. These compositions and abundant fragment peaks of di-HexNAc (406.9 and 407.1) and peaks devoid of di-HexNAc, 1542.1 and 1542.2, indicate these *N*-glycans which include GalNAc–GlcNAc units instead of Gal–GlcNAc units in their outer arms. After sequential partial digestion, elution positions of both *N*-glycans on the two-dimensional map coincided with 110.4a GalNAcβ1,4-GlcNAcβ1,2-Manα1,3-(Manα1,6-)Manβ1,4-GlcNAcβ1,4-(Fucα1,6-)GlcNAc which confirmed from a previous study combining HPLC, NMR and methylation analyses[31]. The elution position on the amide column was smaller than the one of a similar structure, 110.4, which includes Galβ1,4–GlcNAc units in their outer arms[25]. Based on these results, the final form of *N*-glycan digested partially was assigned as 110.4a, and elution positions and suggested structures of digested *N*-glycans A and C are shown in Fig. 8. This indicated that NANA of *N*-glycan A and Fuc of *N*-glycan C was attached to the same α3Man branch of the outer arm and di-HexNAc is GalNAcβ1,4–GlcNAc[31]. The NANA to GalNAc linkage was determined to be α2,6 based on an observed reduction in GU on the amide column[27]. α2,3 NeuAc was reduced to about 0.5 GU on the amide column; on the other hand α2,6 NeuAc increased by about 0.2 GU on the amide column according to the two-dimensional mapping technique[32,33]. The linkage of Fuc in the outer arm of *N*-glycan C was determined to be

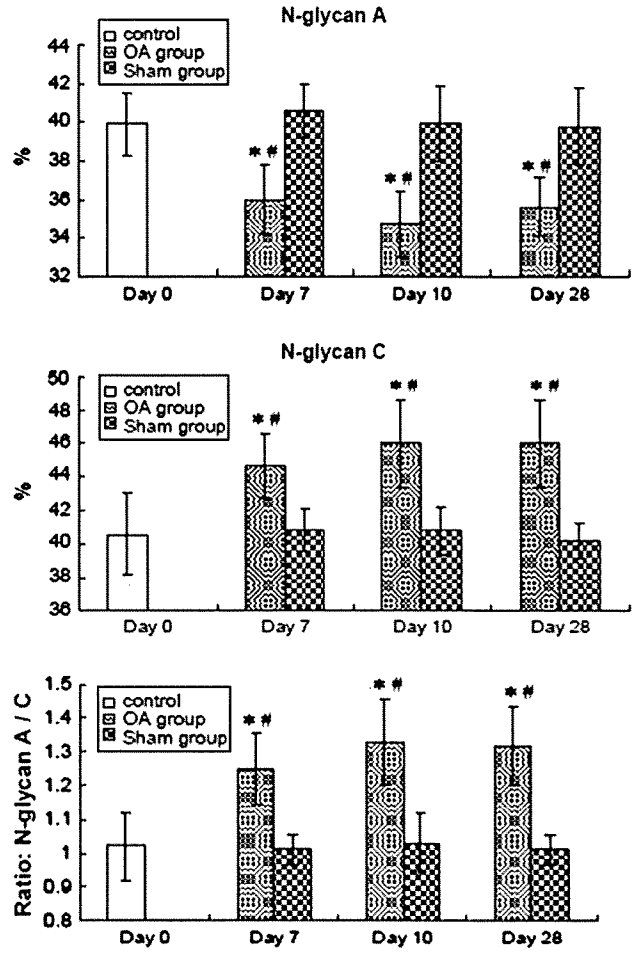

Fig. 5. The ratio in the peak area of *N*-glycans related to OA. Values are means ± SD. The mean ratio of *N*-glycan A decreased significantly from 7 days in the OA group. The mean ratio of *N*-glycan C increased significantly from 7 days in the OA group. The mean ratio of *N*-glycan A–C increased significantly from 7 days in the OA group. *Denotes statistical significance ($P < 0.05$) vs sham group. #Denotes statistical significance ($P < 0.05$) vs control.

an α1,3 linkage to GlcNAc because it was digested with α3/4-Fase and the GalNAc bound to 4 position of GlcNAc. Changing of elution positions with partial digestion is already confirmed in a previous report[32,33]. In this way, structures of *N*-glycans A and C were finally determined as in Fig. 9.

Discussion

The goal of this study was to determine potential alterations in cartilage *N*-glycans with aggravated OA. We first showed alterations in the *N*-glycan peak pattern of articular cartilage between normal rabbit cartilage (sham group) and OA cartilage induced by ACLT (OA group). Then, by comparing peaks obtained from both groups, we showed that the composition of cartilage *N*-glycans was significantly altered in the OA group prior to apparent histological changes. This observation indicates that *N*-glycan alterations in cartilage occur at very early phases of OA aggravation. It is well known that alterations in *N*-glycans are associated with specific disease-related mechanisms[12,13,15]. Several studies of rheumatic diseases report

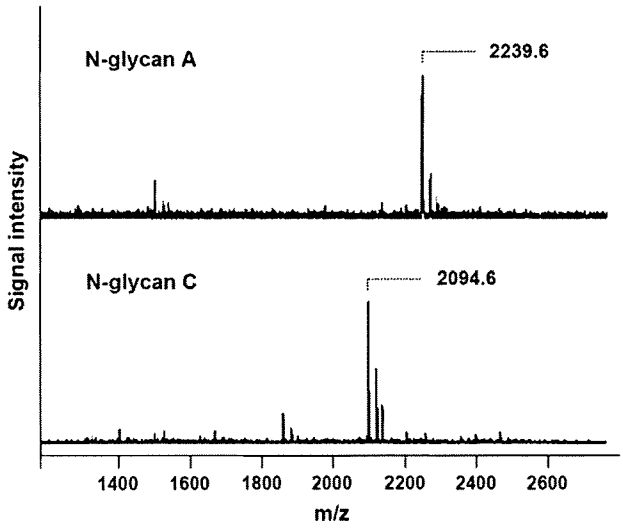

Fig. 6. MALDI-TOF mass spectra. Mass spectrometric analysis of *N*-glycans A and C by the MALDI-TOF/TOF method using DHB as a matrix.

alterations in the *N*-glycan pattern of serum IgG[19–21]. However, little attention has been given to similar alterations in articular cartilage. OA, a chronic degenerative joint disease characterized by articular cartilage deterioration and damage to subchondral bone, is a major cause of disabilities affecting patients' daily activities. Unlike RA, OA is primarily considered a local disease caused by abnormal loading on the articular cartilage. Therefore, analysis of cartilage *N*-glycans may facilitate the understanding of OA pathogenesis. To our knowledge, this is the first study to determine the structure of cartilage *N*-glycans and show alterations in the composition of the cartilage *N*-glycans with OA aggravation.

In early stages of OA aggravation, the macromolecular structure of the ECM is disrupted[5]. Early in this process, chondrocytes begin secreting enzymes that can disrupt ECM macromolecules[1,2]. In particular these enzymes decrease proteoglycan aggregation and concentration of

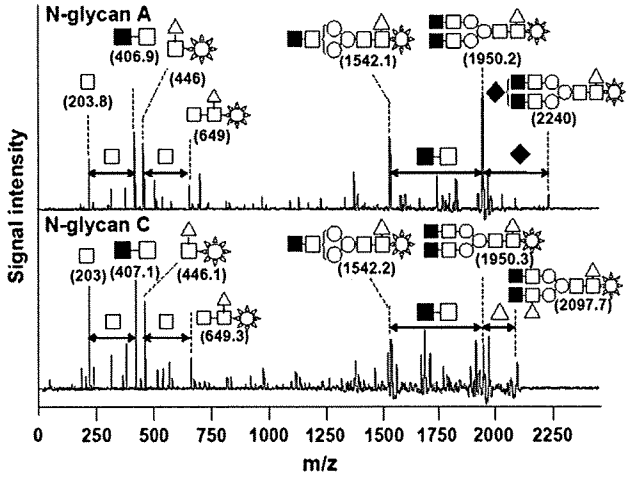

Fig. 7. MALDI-TOF/TOF mass spectra. Structural analysis of *N*-glycans A and C by the MALDI-TOF/TOF method using DHB as a matrix. Structures of fragments of *N*-glycan in each peak are indicated. Mannose, ○; Fuc, △; GalNAc, ■; GlcNAc, □; NANA, ◆; PA, ☼.

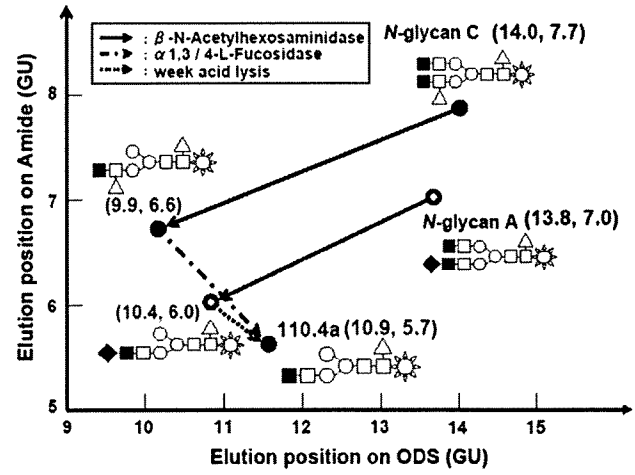

Fig. 8. Structural characterization of *N*-glycans A and C by a combination of exoglycosidase digestion and two-dimensional mapping. A portion of *N*-glycans A and C was digested with exoglycosidases. The elution times on ODS and amide-silica columns of *N*-glycans and their exoglycosidase digests are plotted on a two-dimensional sugar map (expressed as GU). Arrows indicate the direction of changes in the coordinates of *N*-glycans A and C after digestion with: → β-*N*-acetylhexosaminidase, ····▸ α1,3/4-fucosidase, – ▸ weak acid lysis.

cartilage ECM, and their release is accompanied by an increased rate of chondrocyte apoptosis in areas of cartilage regeneration. Our analysis indicates that cartilage *N*-glycans undergo changes in the early phases of OA aggravation. *N*-glycans are abundant on the cell surface and in the ECM, and they commonly interact with protein receptors known as lectins. Through this interaction, *N*-glycans mediate cell–cell and cell–ECM interactions and intra- and extracellular signaling. The current study showed alteration in the representation of two kinds of *N*-glycan whose branch has sialic acid and fucose. Although we suppose that these *N*-glycans relate to OA initiation or progression in early phase, their biological functions remain unclear. Further studies will be performed to elucidate their functional roles in OA progression. Therefore, alterations in the composition of 1A1-210.4b (*N*-glycan A) and 210.41b (*N*-glycan C), whose structures are identified here, likely play crucial roles in the response of chondrocytes or

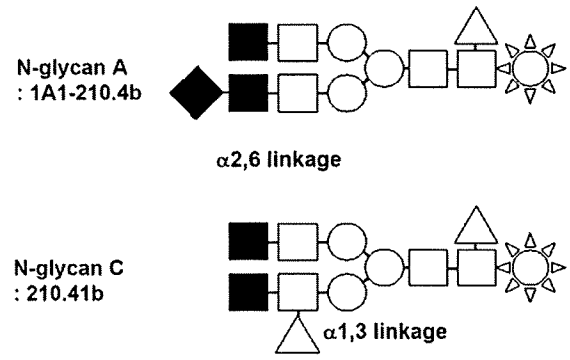

Fig. 9. Structure of *N*-glycans A and C. Indicated are structures of *N*-glycans related to OA. Mannose, ○; Fuc, △; GalNAc, ■; GlcNAc, □; NANA, ◆; PA ☼.

the ECM to changes in the cartilage environment responsible for initiating OA. Here, we did not identify the localization of these *N*-glycans. Future studies are required to determine the biological roles of *N*-glycans identified here in early phases of OA. We observed no significant alterations in the serum *N*-glycan pattern with OA aggravation. Watson *et al.*[20], however, showed alterations in the *N*-glycan pattern of serum IgG with rheumatic diseases, including RA, systemic lupus erythematosus, ankylosing spondylitis, Sjögren's disease, juvenile chronic arthritis, and psoriatic arthritis. In addition to RA, Parekh *et al.*[21] analyzed the *N*-glycan pattern of serum IgG in patients with primary OA and showed that IgG isolated from patients with primary OA contained different distributions of bi-antennary complex-type *N*-glycans. They concluded that primary OA may be a disease related to changes in intracellular processing of *N*-glycans or in their post-secretory degradation. Differences between their results and ours may be due to differences in the *N*-glycan source, to serum or purified IgG, or to mechanisms that induce OA disease. Our current model is a secondary OA model, in which disease is caused by joint instability. Pathological changes must be localized in tissues constituting the joint with cartilage deterioration. Therefore, we conclude that alterations in the *N*-glycan pattern occur in cartilage, not in serum. The results obtained from analysis of both serum and cartilage confirm that OA aggravation following joint instability mainly results from local pathogenesis.

These results and analytical methods can now be applied to clinical studies. The *N*-glycan pattern of articular cartilage may be used as a diagnostic indicator of OA or a predictable indicator of disease aggravation. Although we focus on early phases of OA aggravation, the *N*-glycan pattern of articular cartilage obtained from rheumatic diseases and at advanced stages of OA should now be addressed. By comparing these results, the utility of the *N*-glycan pattern as disease indicators will be established. Also, it is likely that 1A1-210.4b (*N*-glycan A) and 210.41b (*N*-glycan C) identified here play crucial roles in regulating cartilage deterioration following joint instability, but the localization and functional roles of these *N*-glycans are unknown. We are now determining the identities of proteins with specific *N*-glycan structures. When that analysis is complete, we will use knock-out or knock-down of either glycosyltransferase genes or the carrying proteins, followed by a functional analysis of *N*-glycans to further analyze their roles in cartilage deterioration. Finally, the *N*-glycan pattern likely depends on species. For this analysis we used rabbit cartilage, but *N*-glycans altered in human OA cartilage may differ from the *N*-glycans identified here. Thus, the *N*-glycan pattern of degenerative articular cartilage in humans will be analyzed in future studies.

Based on results presented here, we predict that *N*-glycans of human cartilage will alter with cartilage deterioration in diseases such as OA and RA. We will likely observe changes in the linkage of saccharides such as sialic acid and fucose, which is attached to the outer arm of *N*-glycan. Complex combinations of glycosyltransferases and glycosidases control *N*-glycan composition. Therefore, further analysis of expression of glycosyltransferases and glycosidases related to cartilage *N*-glycans should lead to elucidation of the pathogenesis of these diseases.

Regarding the biological and biochemical functions of *N*-glycans obtained in this study, we cannot study any further rabbit model. The reason is that DNA sequences of glycosyltransferases and glycosidases related with cartilage *N*-glycans of rabbit are little known. In our future studies, using human cartilages and conditional model mice, we should determine the functional roles of the *N*-glycans. This should lead to a novel strategy for the treatment of OA.

Recent studies suggest that changes in glycosylation, defined as the addition of sugars to proteins and lipids, have a direct role in the etiology of various diseases, including congenital disorders of glycosylation, von Willebrand factor deficiency, rheumatic diseases, cancers, and emphysema[12,13,19,20,28–30]. Regarding joint diseases, ours is the first study to determine the structure of the cartilage *N*-glycans and analyze potential alterations in damaged cartilage and may provide diagnostics and further insight into OA pathogenesis.

Conflict of interest

The authors have no conflict of interest.

Acknowledgments

We thank Ms Satomi Kudo very much for excellent technical assistance.

References

1. Goldring MB. The role of the chondrocyte in osteoarthritis. Arthritis Rheum 2000;43:1916–26.
2. Bluteau G, Conrozier T, Mathieu P, Vignon E, Herbage D, Mallein-Gerin F. Matrix metalloproteinase-1, -3, -13 and aggrecanase-1 and -2 are differentially expressed in experimental osteoarthritis. Biochim Biophys Acta 2001;1526:147–58.
3. Hamerman D. Aging and osteoarthritis: basic mechanism. J Am Geriatr Soc 1993;4:760–70.
4. Quasnichka HL, Anderson-MacKenzie JM, Tarlton JF, Sims TJ, Billingham ME, Bailey AJ. Cruciate ligament laxity and femoral intercondylar notch narrowing in early-stage knee osteoarthritis. Arthritis Rheum 2005;52:3100–9.
5. Malfait AM, Liu RQ, Ijiri K, Komiya S, Tortorella MD. Inhibition of ADAM-TS4 and ADAM-TS5 prevents aggrecan degradation in osteoarthritic cartilage. J Biol Chem 2002;277:22201–8.
6. Dai SM, Shan ZZ, Nakamura H, Masuko-Hongo K, Kato T, Nishioka K, *et al.* Catabolic stress induces features of chondrocyte senescence through overexpression of caveolin 1: possible involvement of caveolin 1-induced down-regulation of articular chondrocytes in the pathogenesis of osteoarthritis. Arthritis Rheum 2006; 54:818–31.
7. Kouri JB, Rojas L, Perez E, Abbud-Lozoya KA. Modifications of Golgi complex in chondrocytes from osteoarthritic (OA) rat cartilage. J Histochem Cytochem 2002;50:1333–40.
8. Bluteau G, Gouttenoire J, Conrozier T, Mathieu P, Vignon E, Richard M, *et al.* Differential gene expression analysis in a rabbit model of osteoarthritis induced by anterior cruciate ligament (ACL) section. Biorheology 2002;39:247–58.
9. Varki A. Biological roles of oligosaccharides: all of the theories are correct. Glycobiology 1993;3:97–130.
10. Wong CH. Protein glycosylation: new challenges and opportunities. J Org Chem 2005;70:4219–25.
11. Kobata A. Structure and function of the sugar chains of glycoprotein. Eur J Biochem 1992;209:483–501.
12. Yamashita K, Ideo H, Ohkura T, Fukushima K, Yuasa I, Ohno K, *et al.* Sugar chains of serum transferrin from patients with carbohydrate deficient glycoprotein syndrome. Evidence of asparagine-N-linked oligosaccharide transfer deficiency. J Biol Chem 1993;268:5783–9.
13. Wang X, Inoue S, Gu J, Miyoshi E, Noda K, Li W, *et al.* Dysregulation of TGF-β1 receptor activation leads to abnormal lung development and emphysema-like phenotype in core fucose-deficient mice. Proc Natl Acad Sci U S A 2005;102:15791–6.
14. Wacker M, Linton D, Hitchen PG, Nita-Lazar M, Haslam SM, North SJ, *et al.* N-linked glycosylation in *Campylobacter jejuni* and its functional transfer into *E. coli.* Science 2002;298:1790–3.
15. Jaeken J, Carchon H. Congenital disorders of glycosylation: the rapidly growing tip of the iceberg. Curr Opin Neurol 2001;14:811–5.
16. Landberg E, Pahlsson P, Lundblad A, Arnetorp A, Jeppsson JO. Carbohydrate composition of serum transferrin isoforms from patients

with high alcohol consumption. Biochem Biophys Res Commun 1995; 210:267–74.
17. Reitter JN, Means RE, Desrosiers RC. A role for carbohydrates in immune evasion in AIDS. Nat Med 1998;4:679–84.
18. Xiping W, Julie MD, Shuyi W, Huxiong H, John CK, Xiaoyun W, *et al.* Antibody neutralization and escape by HIV-1. Nature 2003;422:307–12.
19. Chou CT. Binding of rheumatoid and lupus synovial fluids and sera-derived human IgG rheumatoid factor to degalactosylated IgG. Arch Med Res 2002;33:541–4.
20. Watson M, Rudd PM, Bland M, Dwek RA, Axford JS. Sugar printing rheumatic diseases: a potential method for disease differentiation using immunoglobulin G oligosaccharides. Arthritis Rheum 1999;42: 1682–90.
21. Parekh RB, Dwek RA, Sutton BJ, Fernandes DL, Leung A, Stanworth D, *et al.* Association of rheumatoid arthritis and primary osteoarthritis with changes in the glycosylation pattern of total serum IgG. Nature 1985; 316:452–7.
22. Tiraloche G, Girard C, Chouinard L, Sampalis J, Moquin L, Ionescu M, *et al.* Effect of oral glucosamine on cartilage degradation in a rabbit model of osteoarthritis. Arthritis Rheum 2005;52: 1118–28.
23. Nakagawa H, Kawamura Y, Kato K, Shimada I, Arata Y, Takahashi N. Identification of neutral and sialyl N-linked oligosaccharide structures from human serum glycoproteins using three kinds of high-performance liquid chromatography. Anal Biochem 1995;226:130–8.
24. Hase S, Ikenaka T, Matsushima Y. Structure analyses of oligosaccharides by tagging of the reducing end sugars with a fluorescent compound. Biochem Biophys Res Commun 1978;85:257–63.
25. Tomiya N, Awaya J, Kurono M, Endo S, Arata Y, Takahashi N. Analyses of N-linked oligosaccharides using a two-dimensional mapping technique. Anal Biochem 1988;171:73–90.
26. Kurogochi M, Nishimura S-I. Structural characterization of glycopeptides by matrix-dependent selective fragmentation of MALDI-TOF/TOF tandem mass spectrometry. Anal Chem 2004;76:6097–101.
27. Takahashi N, Nakagawa H, Fujikawa K, Kawamura Y, Tomiya N. Three-dimensional elution mapping of pyridylaminated N-linked neutral and sialyl oligosaccharides. Anal Biochem 1995;226: 139–46.
28. Sakuma K, Fujimoto I, Hitoshi S, Tanaka F, Ikeda T, Tanabe K, *et al.* An *N*-glycan structure correlates with pulmonary metastatic ability of cancer cells. Biochem Biophys Res Commun 2006;340:829–35.
29. Peracaula R, Tabares G, Royle L, Harvey DJ, Dwek RA, Rudd PM, *et al.* Altered glycosylation pattern allows the distinction between prostate-specific antigen (PSA) from normal and tumor origins. Glycobiology 2003;13:457–70.
30. Mohlke KL, Purkayastha AA, Westrick RJ, Smith PL, Petryniak B, Lowe JB, *et al.* Mvwf, a dominant modifier of murine von Willebrand factor, results from altered lineage-specific expression of a glycosyltransferase. Cell 1999;96:111–20.
31. Tomiya N, Awaya J, Kurono M, Hanazawa H, Shimade I, Arata Y, *et al.* Structural elucidation of a variety of GalNAc-containing N-linked oligosaccharides from human urinary kallidinogenase. J Biol Chem 1993;268:113–26.
32. Tomiya N, Takahashi N. Contribution of component monosaccharides to the coordinates of neutral and sialyl pyridylaminated *N*-glycans on a two-dimensional sugar map. Anal Biochem 1998;264: 204–10.
33. Takahashi N, Wada Y, Awaya J, Kurono M, Tomiya N. Two-dimensional elution map of GalNAc-containing N-linked oligosaccharides. Anal Biochem 1993;208:96–109.
34. Takahashi N, Tomiya N. Analysis of N-linked oligosaccharides: application of glycoamidase A. In: Muramatsu T, Takahashi N, Eds. Handbook of endoglycosidases and glycoamidases. Boca Raton: CRC Press; 1992: 199–332.
35. <http://www.glycoanalysis.info/>; 1992.
36. Nakagawa H, Deguchi K. Structural analysis of sialyl *N*-glycan using pyridylamination and chromatography followed by multistage tandem mass spectrometry. In: Fukuda M, Ed. Methods in Enzymology. San Diego: Elsevier 2006;415:87–104.

SCIENTIFIC ARTICLE

Radial Overgrowth After Radial Shortening Osteotomies for Skeletally Immature Patients With Kienböck's Disease

Tomoya Matsuhashi, MD, Norimasa Iwasaki, MD, Naomi Oizumi, MD, Hiroyuki Kato, MD, Michio Minami, MD, Akio Minami, MD

Purpose We hypothesized that radial shortening osteotomy (radial shortening) for skeletally immature patients with Kienböck's disease would induce overgrowth of the radius. The purpose of this study was to determine the effect of radial shortening on radial growth in skeletally immature patients with Kienböck's disease and to clarify the relationship between the postoperative growth alterations and the clinical results.

Methods Eight wrists of 8 skeletally immature patients with Kienböck's disease were treated with radial shortening. There were 3 boys and 5 girls, ranging in age from 11 to 18 (mean, 14) years old. All patients presented with open physis and negative ulnar variance. The length of the radial shortening equaled the amount of negative ulnar variance. Clinical assessment was based on the modified Nakamura scoring system. Radiographic assessment, including Lichtman's stages, ulnar variance, carpal height ratio, radial inclination, and volar tilt, was performed before surgery, immediately after surgery, and at follow-up. A difference in ulnar variance of more than 2 mm between these 3 measurements was considered to be overgrowth. Statistical comparisons were performed using paired *t*-tests.

Results At a mean follow-up period of 69 months, the mean clinical score was 19.7 of 21 maximum points, with all wrists rated as excellent. Radiographically, no progression of Lichtman stage was found in any patient. At follow-up, the x-ray and magnetic resonance imaging findings indicated lunate revascularization in all patients. Four of the 8 had overgrowth in the operated radius. On the other hand, other radiographic parameters showed no significant changes at follow-up. The occurrence of postoperative radial overgrowth did not notably affect the clinical scores.

Conclusions The current results suggest the probability of overgrowth of the radius in skeletally immature patients with Kienböck's disease treated with radial shortening. The postoperative radial overgrowth after this osteotomy had no effect on clinical and other radiographic outcomes. *(J Hand Surg 2009;34A:1242–1247. © 2009 Published by Elsevier Inc. on behalf of the American Society for Surgery of the Hand.)*

Type of study/level of evidence Therapeutic IV.

Key words Radial shortening osteotomy, skeletally immature patients, Kienböck's disease, postoperative overgrowth.

From the Department of Orthopaedic Surgery, Hokkaido University Graduate School of Medicine, Sapporo, Japan; Department of Orthopaedic Surgery, Shinsyu University Graduate School of Medicine, Matsumoto, Japan; Hokkaido Orthopaedic Memorial Hospital, Sapporo, Japan.

Received for publication June 24, 2008; accepted in revised form April 20, 2009.

No benefits in any form have been received or will be received related directly or indirectly to the subject of this article.

Corresponding author: Norimasa Iwasaki, MD, Department of Orthopaedic Surgery, Hokkaido University Graduate School of Medicine, Kita 15 Nishi 7, Sapporo, 060-8638, Japan; e-mail: niwasaki@med.hokudai.ac.jp.

0363-5023/09/34A07-0010$36.00/0
doi:10.1016/j.jhsa.2009.04.028

KIENBÖCK'S DISEASE OFTEN affects men between the ages of 20 and 40 who are manual laborers.[1] The pathogenesis of this disease process is still controversial. Consequently, various surgeries, including excision arthroplasty,[2,3] radial wedge and shortening osteotomies,[4–8] limited intercarpal arthrodeses,[9–11] and lunate revascularization procedures[12–14] have been advocated as treatments.

Based on the theory that negative ulnar variance is a potential causative factor in Kienböck's disease,[15,16] radial shortening osteotomy (radial shortening) has been advocated for patients with negative ulnar variance and has been reported to improve clinical results in adults.[4,5,7] However, little is known about the postoperative history of the disease in skeletally immature patients. In a recent study, Iwasaki et al.[6] reported that radial shortening provided satisfactory clinical and radiographic outcomes in teenage patients, even at advanced stages of the disease.

We found few reports concerning the outcome and risk of postoperative overgrowth of the radius after radial shortening for skeletally immature patients in Kienböck's disease.[17]

In this study, we performed radial shortening for skeletally immature patients with Kienböck's disease and evaluated clinical and radiographic results. The hypothesis was that radial shortening for skeletally immature patients with Kienböck's disease would induce alterations in radial growth. The aims of this study were to determine the effect of radial shortening on radial growth in skeletally immature patients with Kienböck's disease and to elucidate relationships between postoperative growth changes and clinical outcomes.

MATERIALS AND METHODS

We retrospectively identified and reviewed all skeletally immature patients with symptomatic Kienböck's disease who were considered for radial shortening from 1990 to 2004. Chart reviews identified 8 patients. Three surgeons carried out radial shortening for the 8 patients with negative ulnar variance. Hospital medical records and preoperative and postoperative radiographs obtained at regular follow-ups were collected in order to evaluate the clinical and radiographic findings. There were 3 boys and 5 girls between 11 and 18 (mean, 14) years old. They presented with open physis. All patients had an occupational or recreational background of repeated minor stress to the wrist. Six patients had a history of acute trauma to the affected wrist. In all patients, occupational or recreational activities were interrupted by severe wrist pain. Preoperative Lichtman's stages[18] were determined according to the radiographic findings (Table 1). In identifying preoperative Lichtman's stages in this study, 2 cases were at stage II, 2 cases were at stage IIIA, and 4 cases were at stage IIIB. All patients had preoperative magnetic resonance imaging (MRI), and 6 of the 8 patients had MRI scans at follow-up.

TABLE 1. Lichtman's Stages

Staging	Radiographic Assessment
Stage I	Normal except for the possibility of a linear or compression fracture
Stage II	Definite changes in the apparent density of the lunate
Stage IIIA	Collapse of the entire lunate at a normal scapholunate angle
Stage IIIB	Collapse of the entire lunate at a scapholunate angle greater than 60°
Stage IV	Generalized degenerative changes in the carpus

Surgical technique

All surgeries on the patients were performed under general anesthesia. An 8-cm longitudinal skin incision was made in the distal part of the anterior aspect of the forearm, parallel and lateral to the tendon of the flexor carpi radialis. The distal part of the radius was exposed between the brachioradialis and the flexor carpi radialis tendon. Radial shortening was carried out by making 2 parallel transverse cuts and removing an appropriate segment of the bone. The length of the removed segment equaled the amount of negative ulnar variance measured on the preoperative radiograph. The osteotomy site was fixed by a 5-hole or 6-hole dynamic compression plate. Using fluoroscopy, we avoided a growth plate injury by plate application. After surgery, a below-elbow splint was applied for 2 weeks. All patients had surgery to remove the plate approximately 1 year after surgery.

Outcome assessment

At follow-up, patients were evaluated clinically and radiographically. Clinical evaluation was based on a modification of the scoring system of Nakamura et al. (Table 2).[19] Three observers examined clinical findings at follow-up. The original scoring system with a 30-point maximum was based on clinical and radiographic results, with 21 points and 9 points, respectively. Although the radiographic assessment was deleted from the original scoring system, we assessed the radiographic findings in other parameters, including ulnar

TABLE 2. Modified Nakamura et al. Scoring System

Clinical Assessment	Points
Pain in the wrist	
None	10
Mild with strenuous activity	7
Mild with light work	4
Grip strength (percentage of unaffected side)	
90%	5
80%	4
70%	3
60%	2
50%	1
Increase in range of flexion and extension	
>20°	6
10° to 19°	5
5° to 9°	3
Overall grade	Total points
Excellent	15–21
Good	9–14
Fair/poor	<8

variance,[15,20,21] carpal height ratio,[3,22] radial inclination,[23] and volar tilt.[23]

Radiographic evaluation was based on the Lichtman stage.[18] The progression of degenerative change through the entire wrist joint and revascularization of the diseased lunate was determined with anteroposterior (AP) and lateral radiographs of the wrist. The radiographic parameters, including ulnar variance,[15,20,21] carpal height ratio,[3,22] radial inclination,[23] and volar tilt,[23] were measured before surgery, immediately after the radial shortening, and at follow-up. The *ulnar variance* is defined as the difference on the AP radiograph between the transverse line at the level of the lunate fossa and the transverse line at the level of the ulnar head, with the shoulder abducted, elbow flexed, and forearm in neutral rotation to quantify variance.[15,20,21] The *carpal height ratio* is defined as the carpal height divided by the length of the third metacarpal on the AP radiograph.[3,22] The *radial inclination* is the angle of the distal radial articular surface to the line perpendicular to the long axis of the radius on the AP radiograph.[23] The volar tilt is the angle created between the articular surface of the distal radius and the line perpendicular to the long axis of the radius on the lateral radiograph.[23] Regarding overgrowth, a difference in length of more than 2 mm was considered a discrepancy.[24] According to the MRI grading system by Nakamura et al,[19] the preoperative and postoperative signal intensities of the lunate were evaluated.

The radiographic measurements were all made by the senior author (N.I.), an experienced hand surgeon. Intra-observer variations in the measurements were assessed by calculating the coefficient variation, which equals the standard deviation divided by the mean value. The observer took 5 measurements of each parameter in the same radiograph. The coefficient of variation of each parameter among the results of 5 sets was calculated. The value was 9% in the ulnar variance, 3% in the carpal height ratio, 4% in the radial inclination, and 9% in the volar tilt. These low values showed a high reliability of the radiographic measurements.

Statistical analysis

All data are represented as mean ± standard deviation. Statistical comparisons were performed using paired *t*-tests. The level of significance was set at $p < .05$.

RESULTS

Clinical assessments

At a mean follow-up of 69 (range, 36–117) months, 6 of the 8 patients were free from pain, and the remaining patients had mild wrist pain on strenuous activity. No patient had pain at the distal radioulnar joint or at the osteotomy site. The mean postoperative range of extension and flexion of the wrist increased significantly, from 91° ± 16° to 151° ± 21° ($p < .01$). The grip strength of the affected side compared with the unaffected side improved from 43% ± 13% to 104% ± 10% ($p < .01$). Based on the scoring system, the mean clinical score was 19.7 (range, 17–21) of 21.0 maximum points. All patients were classified as excellent. There were no postoperative complications.

Radiographic assessments

Bony union at the site of the osteotomy was achieved within 12 weeks in all patients. Radiographic findings suggested that radial shortening prevented disease progression and enhanced diseased lunate revascularization. At follow-up, no progression of Lichtman stages was found in any patient. There were no degenerative changes in the distal radioulnar joint or the radiocarpal joint in any patients. Lunate revascularization, based on the radiographic findings, was found in all patients. Magnetic resonance imaging scans of all patients showed grade V of the Nakamura's grading system, as defined by generalized, low signal intensity of the lunate on T1-weighted and T2-weighted images, before surgery. At follow-up, in 4 of the 6 patients, the MRI

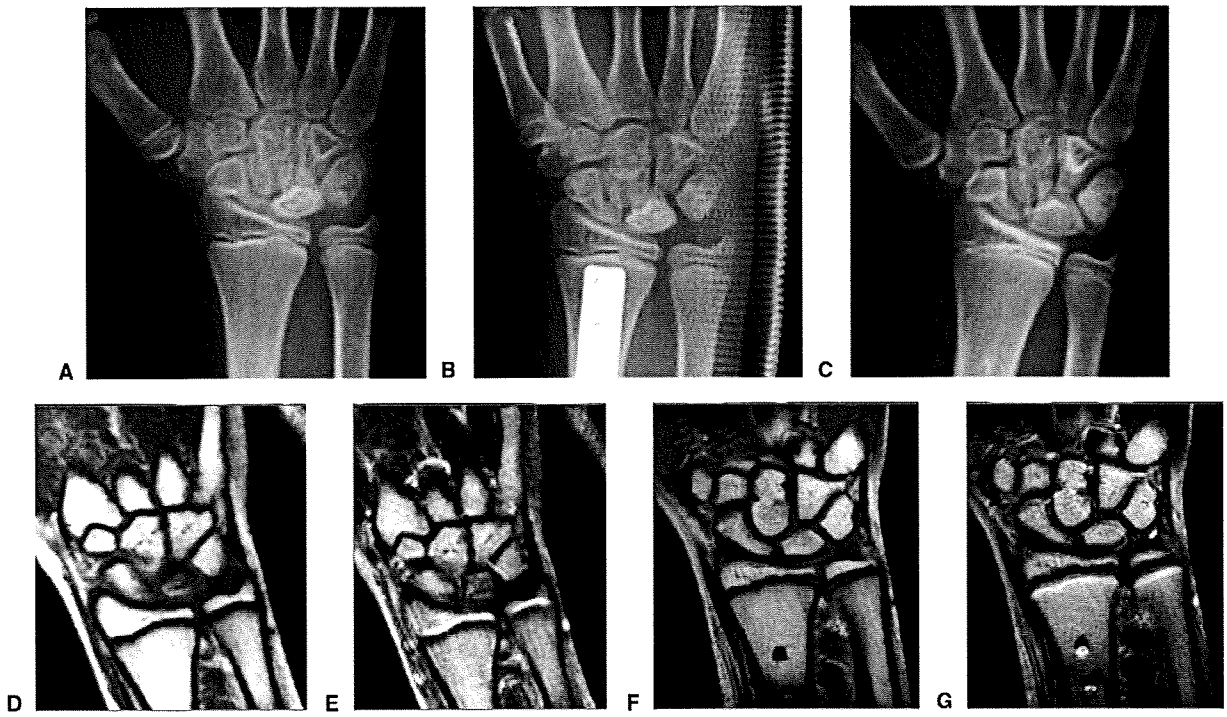

FIGURE 1: A A preoperative AP radiograph of an 11-year-old boy with Stage IIIA Kienböck's disease in the right wrist. **B** The AP radiograph shows ulna-zero variance immediately after radial shortening. **C** The AP radiograph obtained 48 months after radial shortening indicates lunate revascularization with improved appearance of the lunate in density and height. **D, E** Preoperative coronal T1- and T2-weighted MRI images show diffuse decreased signal intensity of the lunate. **F, G** At follow-up, T1- and T2–weighted images demonstrate return of normal signal intensity of the involved lunate.

TABLE 3. Radiographic Parameters

Radiographic Assessment	Before Surgery (Mean ± SD)	Immediately After Surgery (Mean ± SD)	At Follow-Up (Mean ± SD)
Ulnar variance (mm)*	−3.1 ± 1.6	−1.4 ± 1.3	−3.9 ± 2.2
Carpal height ratio	0.47 ± 0.04	0.48 ± 0.04	0.48 ± 0.03
Radial inclination (degrees)	23.8 ± 3.9	23.6 ± 3.9	21.5 ± 4.9
Volar tilt (degrees)	10.0 ± 3.1	8.8 ± 2.6	9.9 ± 3.9

*Denotes statistical significance between "Immediately after Surgery" data and "At Follow-up" data ($p < .05$). Minus numbers refer to negative ulnar variance and positive numbers refer to positive ulnar variance.

scans demonstrated a return of normal marrow signal intensity of the lunate, indicating grade I (Fig. 1). Grade II, including localized regions of slightly decreased signal intensity, was found in the remaining 2 patients.

Postoperative alterations in radiographic parameters showed a tendency toward radial overgrowth after radial shortening for teenagers with Kienböck's disease. Table 3 summarizes the alterations in radiographic parameters. The mean postoperative ulnar variance increased significantly from 1.4 ± 1.3 mm (range, 0–4 mm) of negative ulnar variance to 3.9 ± 2.2 mm (range, 1–8 mm) of negative ulnar variance ($p < .03$). Based on the criteria for overgrowth, 4 of the 8 patients had radial overgrowth on the affected side of the radius (Fig. 2, Table 4). All 4 of these patients were less than 13 years old at the time of surgery. On the other hand, the other parameters showed no notable changes after surgery.

Effect of postoperative radial overgrowth on clinical outcomes

The occurrence of postoperative radial overgrowth did not considerably affect the clinical scores. The mean score was 20.5 ± 0.9 in the patients with radial overgrowth and 19.0 ± 1.6 in those without radial overgrowth.